N62269-79-C-0288 (12)

79-0288

FINAL REPORT FOR CONTRACT N62269-79-C-0288

HOLOGRAPHIC LASER VISOR MOCK-UP

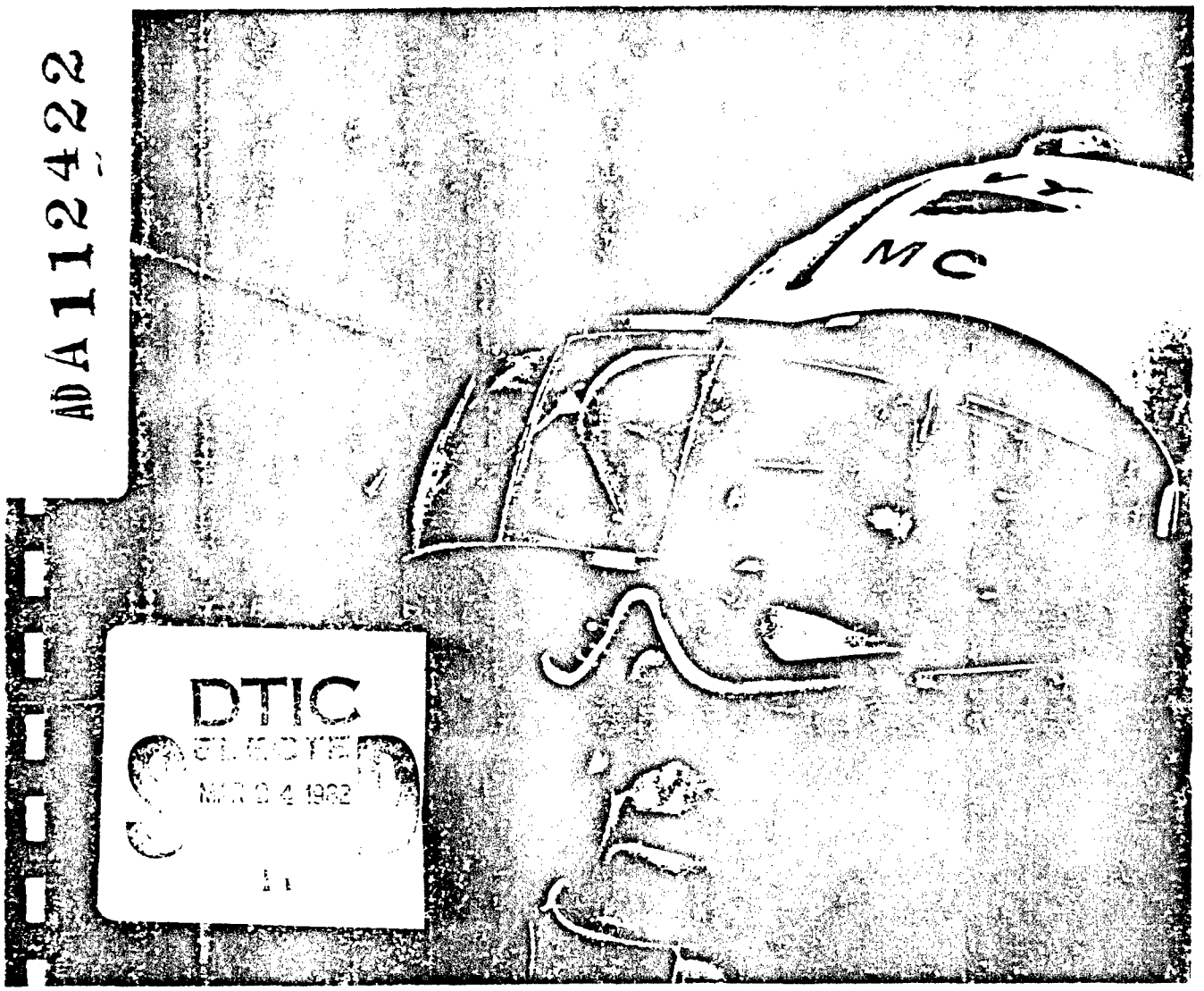

JUNE 1981

PREPARED FOR
NAVAL AIR DEVELOPMENT CENTER
WARMINISTER, PENNA 18974

HUGHES

HAC REF. NO. E6018

Final Report

HOLOGRAPHIC LASER VISOR MOCKUP

June 1981

Prepared by: M. J. Chern
T. L. Dobbs
G. E. Moss

N62269-79-C-0288

Display Systems Laboratory
Radar Systems Group
AEROSPACE GROUPS

Hughes Aircraft Company o El Segundo, California

CONTENTS

CONTENTS (Continued)

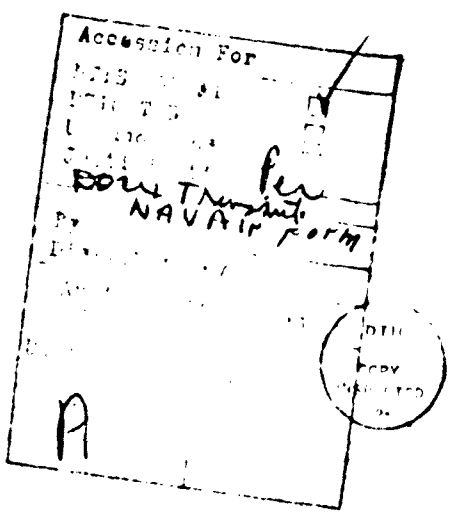

LIST OF ILLUSTRATIONS

LIST OF ILLUSTRATIONS (Continued)

LIST OF ILLUSTRATIONS (Continued)

1.0 PROGRAM DESCRIPTION

1.1 HOLOGRAPHIC REFLECTORS - A NEW APPROACH TO LASER EYE PROTECTION

The goal of this program was to show that a holographic reflector added to a pilot's visor can provide laser eye protection which has advantages over that which can be provided by other means such as the addition of an absorbing dye.

There are already a number of laser systems in field use for applications such as communications, ranging and target designation. Many of these systems emit laser radiation that can damage the eyes of either aircrews or ground personnel in the vicinity. There is also the potential threat that enemy lasers will be developed as weapons for blinding a pilot. A laser eye protection device is needed to protect the eye from these various hazards without interfering with normal vision. Such a device does not now exist.

The current method of protecting a pilot from laser eye damage is to put an absorptive dye into his helmet visor. One disadvantage of this method is that the dye absorbs a wide band of wavelengths. This wideband absorption both darkens and tints the scene that is viewed. The effective visual degradation is unacceptable for critical applications such as piloting.

This degradation can be reduced by replacing the dye with a holographic mirror which selectively reflects a narrow wavelength spectrum. Being more wavelength selective, holographic rejection provides improved see-through.

It was the objective of this contract to build a visor segment sample and several other sample holograms to demonstrate that the holographic method can achieve the required eye protection. Specific tasks were to fabricate and test the following:

1) A 2 in. x 8 in. holographic reflector mounted in a simulated visor segment to demonstrate see-through characteristics (Figure 1).
2) A sample hologram to demonstrate rejection of 1.06 μm radiation (Figure 2).
3) A sample double hologram to demonstrate a method of increasing angular coverage which would reduce the distance needed between the eye and the hologram (Figure 2).
4) A sample two layer hologram to demonstrate simultaneous rejection of radiation at two wavelengths: 1.06 μm and a wavelength in the visible region (Figure 2).

The design, construction, and performance evaluation of these various holographic elements is described on the following pages. The results show that a holographic reflection element can provide laser eye protection with less degradation of normal vision than other methods.

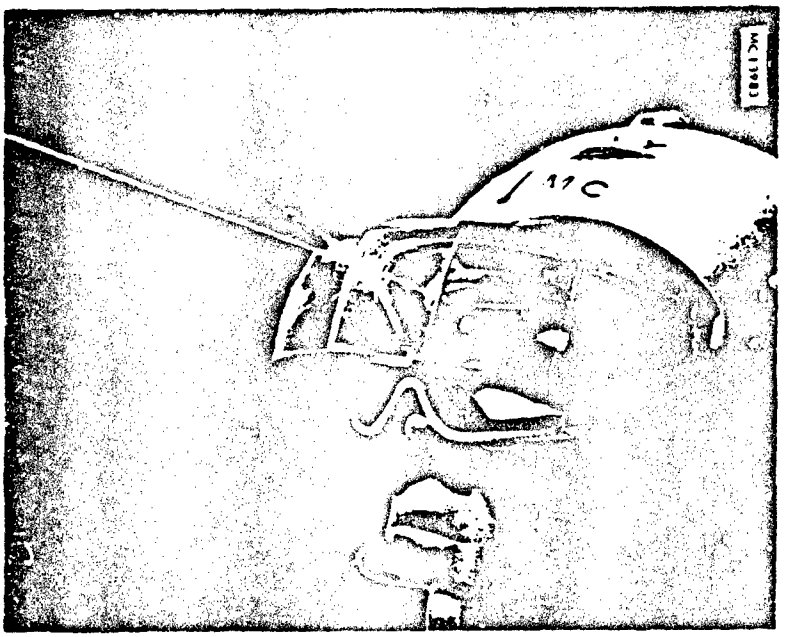

Figure 1. Holographic laser eye protection visor

Figure 2. Holographic visor and other sample holographic elements

1.0 PROGRAM DESCRIPTION

1.2 RESULTS SHOW THAT HOLOGRAPHIC REFLECTORS CAN PROTECT THE EYE

The holographic reflectors developed on this program achieved 99.999% reflection of 530 nm radiation with photopic see-through of 80%, 99.99% reflection of 1.06 μm radiation, and better than 99.9% rejection for both wavelengths of the two-layer hologram.

The primary task was to design and construct a segment of a visor to demonstrate the effectiveness of holographic laser eye protection. It was found that the angular coverage of a single hologram was not enough to protect both eyes of a wearer. Therefore, two holographic reflectors were superimposed in the same visor with one protecting each eye as shown in Figure 3. In order to simplify the construction optics for the sample visor it was made in four smaller pieces which were then assembled in a frame to wear for evaluation. Each of the four hologram pieces consists of a sealed together inner and outer substrate with a hologram made on both bonded surfaces.

The rejection for a particular visible wavelength of one of these reflector elements is shown on the angle vs. diffraction efficiency curve in Figure 4. Notice that for an angular coverage of 39^{0} the rejection is better than 99.9%. 39 degree angular coverage is sufficient to protect all persons in the 5 to 95 percentile eye spacing range. The rejection level of 99.9% minimum was chosen as a goal for a useful protection device. The other three tasks in this program were successful in demonstrating rejection capability of other types of reflection holograms.

A single 1.06 μm hologram had a peak rejection of 99.8%. As shown in Figure 5, two of these holograms bonded together rejected more than 99.99%. The single 1.06 μm efficiency was lower than expected because of spurious holograms generated by the extremely high construction angles that were used in these sample devices.

A sample double-skew hologram increased the angular rejection range from 38 to 66.5 degrees. This can decrease the eye-to-visor distance from 54 mm to 28 mm with no loss in eye protection.

A sample two wavelength hologram demonstrated the ability of the holographic rejection method to add holographic mirrors on the same surface. In principle any number of wavelengths can be rejected with the only effect being loss of photopic see-through as each slice of the visible region is removed.

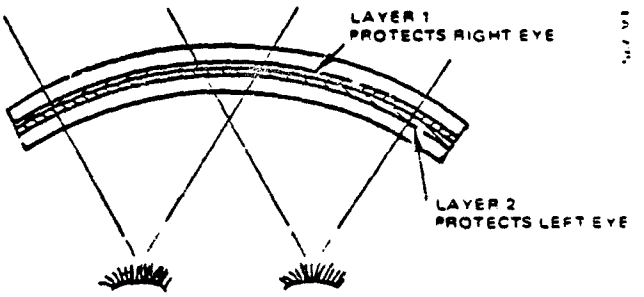

Figure 3. Two layer visor

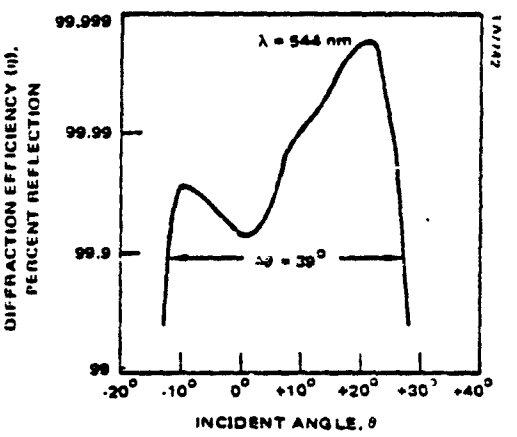

Figure 4. Hologram efficiency vs incident angle for visor segment "A"

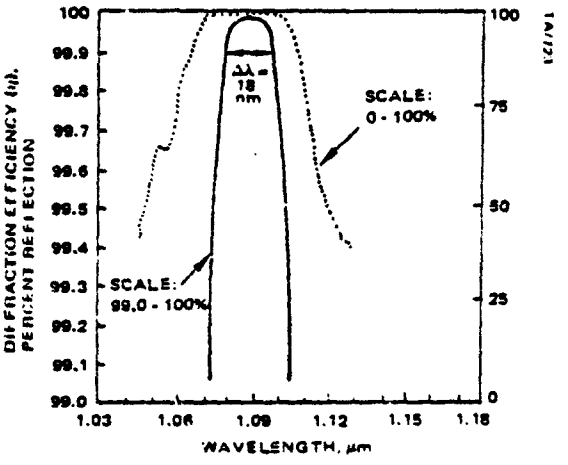

Figure 5. Sample 1.06μm reflector

1.0 PROGRAM DESCRIPTION

1.3 ADVANTAGES OF THE HOLOGRAPHIC APPROACH

A holographic reflector has two chief advantages over other devices for protecting the eye from laser radiation. These are: 1) a narrow band of wavelengths can be rejected without appreciably attenuating the rest of the spectrum, 2) the shape of the holographic reflector can be made relatively independent of the reflector function.

A fundamental problem with using dye absorption to protect against laser radiation is that dyes absorb a wide band of wavelengths. In contrast, an advantage of using a holographic reflector is that it is inherently a narrow-band device. This is because it works by adding the in-phase reflections from a number of recorded layers of varying index of refraction. Only at particular wavelengths and angles does the radiation add up in phase to reflect from the hologram. Other wavelengths and angles pass through the holographic reflector unattenuated providing clear see-through except at the reflection wavelength desired. As shown in Figure 6, the 20 nm reflection bandwidth of a typical holographic reflector is contrasted with the very wide absorption bandwidth of a typical dye. In actual practice, as will be seen in this report, the design of the holographic reflector is complicated by the need to provide eye protection over a wide range of angles. These angles correspond to the area of eye location to be protected when viewed from a point on the holographic reflector. Sometimes, the angular protection range needed will be seen to require more than one holographic reflector for full coverage.

Another advantage of using the holographic approach is that to protect against any chosen wavelength a device can be made from the same recording material. The hologram can be recorded at some convenient wavelength and then chemically processed to shift it to the desired wavelength. This ability to tailor one recording material to any wavelength contrasts with the need in the dye absorption method to develop different dyes to absorb different wavelengths.

Another advantage of the holographic reflector is its relative independence of shape. A diffraction optics element can be recorded so that its reflecting fringe layers are at an arbitrary angle within the recording film. This contrasts with other multilayer devices such as optical coatings in which the layers can be deposited only parallel to the substrate surface. For these devices, the fact that the layers are parallel to the surface restricts the visor shape to that needed for the filter.

A comparison between eye protection devices using a multilayer coating and a diffraction optics reflector is shown in Figure 7. Notice that, to provide protection, the multilayer coating must be concentric around each eye which requires a "bugeye" shaped visor. The holographic reflector, however, can adapt to a more standard visor shape. As shown, the holographic visor consists of separate reflectors recorded to protect each eye.

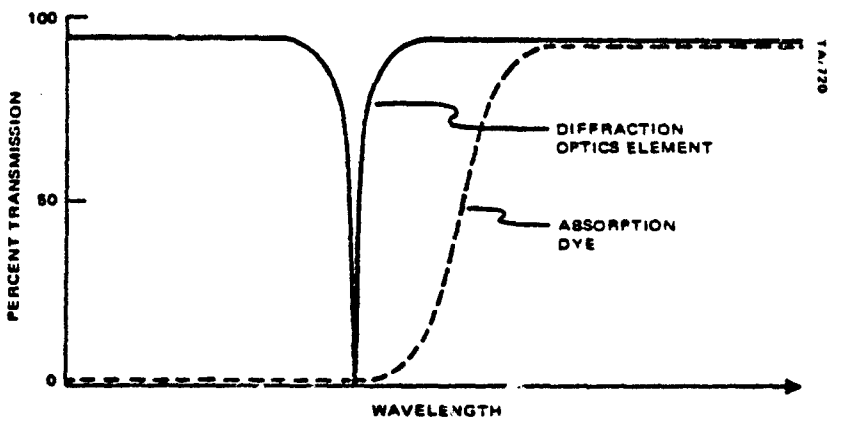

Figure 6. Narrowband diffraction optics vs broad absorption dye

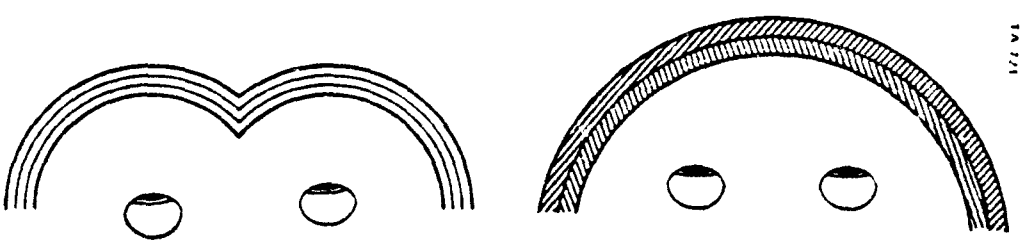

a. Multilayer conventional coating

b. Double diffraction optics coating

Figure 7. Comparison of coatings

2.0 THEORETICAL ANALYSIS

2.1 THEORETICAL ANALYSIS OF HOLOGRAM PERFORMANCE PROVIDES GUIDELINES FOR REALISTIC VISOR DESIGN

An optimum visor design can only be achieved with thorough understanding of the hologram performance. The coupled wave theory developed by Kogelnik is used to predict the various parameters pertinent to the laser visor applications.

As stated in the previous section, a hologram may be utilized to provide high rejection at a specific laser wavelength and still maintain high photopic transmission for easy see-through. To design such a holographic visor, thorough understanding of the hologram properties is required. Therefore, we will analyze the hologram properties to predict the potential, limitation, and trade-off factors.

The properties of various types of holograms have been analyzed by many authors. For the laser eye protection visor application, the high efficiency hologram of the reflection type is of particular interest to us. In this report, the efficiency is defined as the fraction of energy not transmitted through the hologram. Because of the high efficiency, the incident energy is depleted rapidly and is reflected as it propagates through the hologram layer. The coupled wave theory developed by Kogelnik takes into account the strong interaction between the incident radiation and the deflected radiation. Therefore, we will follow Kogelnik's approach for theoretical analysis of the hologram properties.

For the purpose of analysis, the geometry of a hologram is shown in Figure 8. The recorded fringe planes are spaced at a distance Λ apart and are oriented at angle ϕ with respect to the hologram boundary. This slant angle ϕ is less than 45° for the reflection type hologram. The incident radiation with wavelength λ impinges on the hologram at an angle θ in air, and θ_2 in the holographic medium with thickness D. The index of refraction in the medium changes sinusoidally as expressed by $n = n_o + \Delta n \sin kx$, Δn is called the index modulation. The fringe planes schematically represent areas of either highest or lowest index of refraction. The recording medium used for this contract is dichromated gelatin which shows almost no absorption in the visible and near IR region. It is reasonable to assume that we are dealing with a non-absorbing medium.

For a non-absorbing reflection hologram, Kogelnik's coupled wave theory leads to a general formula for diffraction efficiency, Equation (1). This equation relates the hologram properties such as peak efficiency, spectral response, angular dependence, etc., to a number of physical hologram parameters (D, Δn, Λ, n, etc.). Furthermore, the photopic transmission of the hologram can be calculated using Equation (2). Here $\eta(\lambda)$ is the rejection efficiency of the hologram at wavelength λ, and $[1-\eta(\lambda)]$ is the tranmission of the hologram. $V(\lambda)$ is the CIE standard visibility factor for the human eye response. Equations (1) and (2) are the basis of all analytical cacluations in this report.

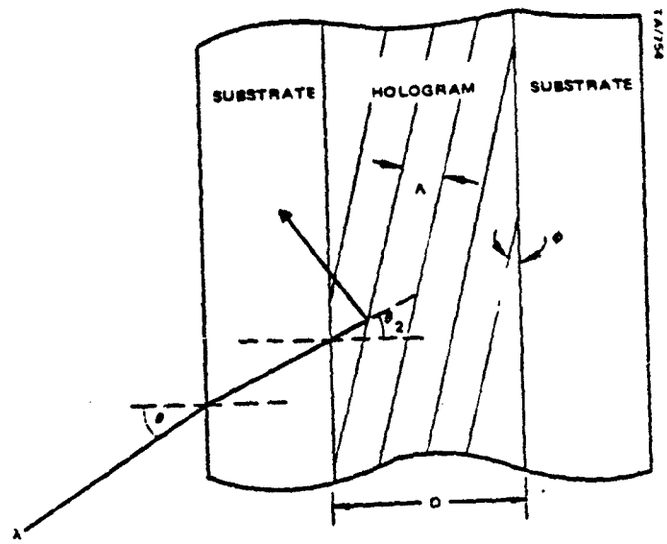

EQUATION (1): DIFFRACTION EFFICIENCY

$$\eta(\lambda,\theta) = 1/\left\{1 + (1 - \xi^2/\nu^2)/\mathrm{Sinh}^2\ \sqrt{\xi^2 - \nu^2}\right\}$$

WHERE $\nu = \pi \cdot \Delta n \cdot D/(\lambda\sqrt{C_S \cdot \cos\theta})$

$$\xi = \pi \cdot D \cdot (\cos(\phi - \theta) - \lambda/(2n\Lambda))/(\Lambda \cdot C_S)$$

$$C_S = \lambda\cos\phi/(\Lambda \cdot n) - \cos\theta$$

EQUATION (2): PHOTOPIC TRANSMISSION

$$T = [\int V(\lambda)\,[1 - \eta(\lambda)]\,d\lambda]/[\int V(\lambda)\,d\lambda]$$

V(λ): VISIBILITY RESPONSE OF HUMAN EYE

Figure 8. Hologram geometry for analysis

2.0 THEORETICAL ANALYSIS

2.2 RESULTS OF THEORETICAL ANALYSIS

Theory predicts that a high efficiency hologram for .53 μm laser radiation can provide a minimum of 99.9% rejection over an angular span of 36 degrees and still maintain 80% photopic transmission.

Using the coupled wave theory (Eq. 1 and Eq. 2), properties of a hologram can be numerically calculated. There are several properties especially important to the use of a hologram as a laser eye protection visor. These properties include peak efficiency (η_o), angular protection range ($\Delta\theta$), and the photopic transmission (T). The angular protection $\Delta\theta$ is the angular range within which the hologram efficiency is better than a certain pre-determined minimum requirement. The photopic transmission is the see-through level corrected by the human eye response $V(\lambda)$.

For the purpose of illustrating the essential characteristics of a hologram, the following conditions are assumed for the calculations:

1) the incoming laser radiation wavelength is .53μm
2) minimum rejection efficiency requirement is 99.9% or optical density OD = 3.0
3) the hologram fringes are parallel to the substrate surface, i.e., $\phi = 0^o$.

The theory predicts that the modulation factor $\Delta n*D$ is the most critical parameter for achieving high efficiency.

Figure 9 shows the relationship of peak efficiency η_o as a function of $\Delta n*D$. To achieve high peak efficiencies of 99.9% or better, $\Delta n*D$ has to be .70 or higher. The higher the peak efficiency, the larger the protection angle $\Delta\theta$ as shown in Figure 10. It is interesting to note that for holograms with the same peak efficiency, the angular protection $\Delta\theta$ increases as the hologram layer thickness D decreases. This is a consequence of the wavelength bandwidth narrowing as the thickness of a multilayer dielectric interference structure increases. Therefore to obtain maximum $\Delta\theta$, it is desirable to fabricate a hologram with maximum Δn at the same thickness.

As the peak efficiency goes beyond the minimum requirement of OD = 3.0, the angle $\Delta\theta$ increases rapidly. For further improvement in the peak efficiency beyond about OD = 4.0, the angle $\Delta\theta$ increases at a slower rate. Thorough calculations indicate that $\Delta\theta = 35^o$ to 40^o is probably a good practical limit of a single hologram with typical thickness at about 14-16um. When the incident beam is propagating along a direction perpendicular to the fringe planes, the efficiency is maximum at the wavelength λ_H which is twice of the fringe spacing Λ in the medium, ie. $\lambda_H = 2n\Lambda$. The wavelength λ_H, called the hologram wavelength, is one of the physical characteristics of the hologram.

The photopic transmission, T, (Figure 11) of a hologram in the visible region decreases as the peak efficiency of the hologram increases The decrease is due to the broadening of the reflection spectral bandwidth as the peak efficiency goes up. For the same efficiency, a thicker hologram gives a higher transmission. Therefore, there is a trade-off between $\Delta\theta$ and T when determining the necessary hologram thickness.

Another consideration in the use of a hologram as a protection visor is "how does $\Delta\theta$ change when the hologram wavelength, λ_H, drifts as function of time?" The result of calculations, Figure 12, indicate that $\Delta\theta$ decreases significantly as λ_H changes for a hologram with marginal efficiency. However, for a hologram with high efficiency, deviation from the laser wavelength may increase the protection angle. Overall, it is crucial to control precisely the hologram peak wavelength with respect to the laser wavelength.

To further illustrate this relationship, numerical calculations are done for a hologram with peak efficiency OD = 4.0, thickness D = 18 µm, and laser wavelength .53µm. The changes of $\Delta\theta$ for OD = 3.0 protection of the laser radiation as the hologram wavelength drifts are shown in Figure 13. The OD = 4.0 hologram provides up to 36^0 protection when the hologram wavelength is at .536µm. The $\Delta\theta$ decreases to 30^0 when the hologram wavelength coincides with the laser wavelength at .53µm. The photopic transmission is 80% at 536µm, and it increases slightly as the hologram wavelength drifts down further away from the peak photopic response at .555µm.

In a practical hologram, the hologram wavelength across the hologram area may differ due to the fabrication process. The peak protection wavelength will drift as function of time due to the inherent instability. Certain wavelength tolerance ($\Delta\lambda$) should be allowed for a useful visor. Results shown in Figure 13 indicate that $\Delta\lambda$ = 5nm is allowed for a visor requiring minimum $\Delta\theta$ of 30^0.

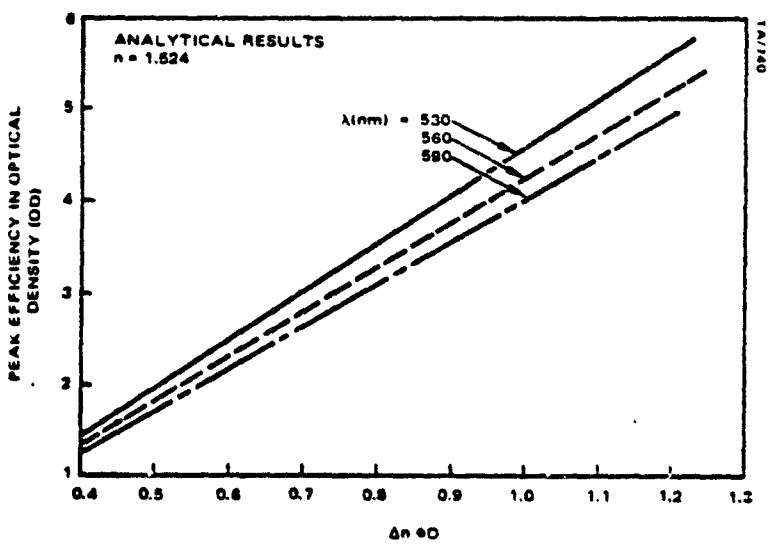

Figure 9. Peak efficiency vs modulation factor ($\Delta n.D$)

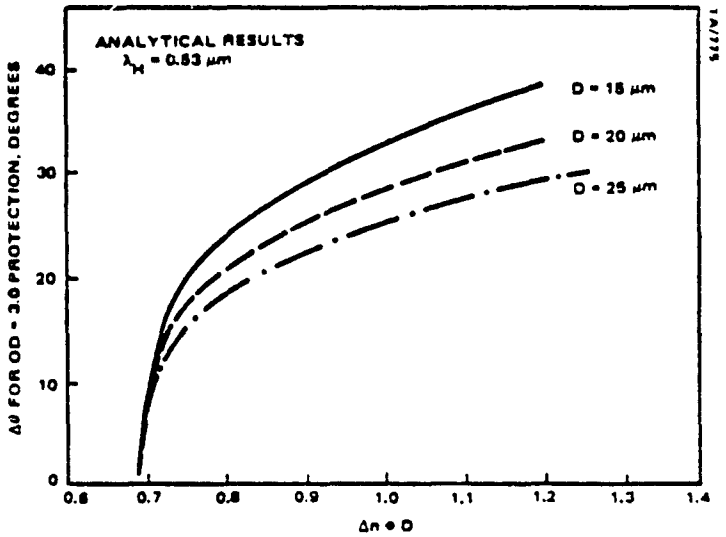

Figure 10. Protection angle ($\Delta\theta$) vs modulation factor ($\Delta n \cdot D$)

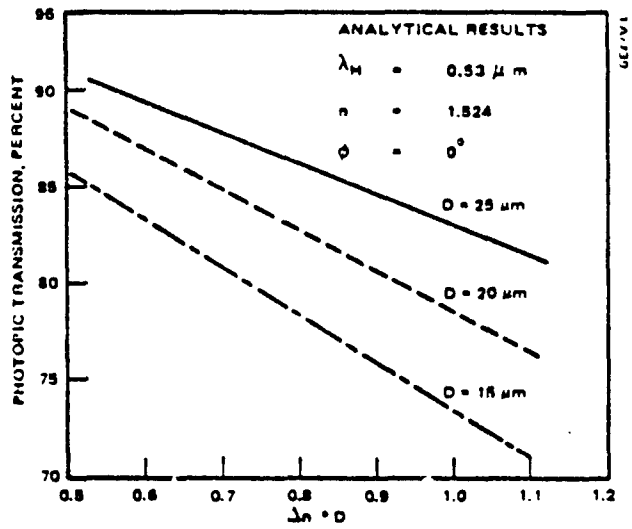

Figure 11. Photopic transmission vs modulation factor ($\Delta n \cdot D$)

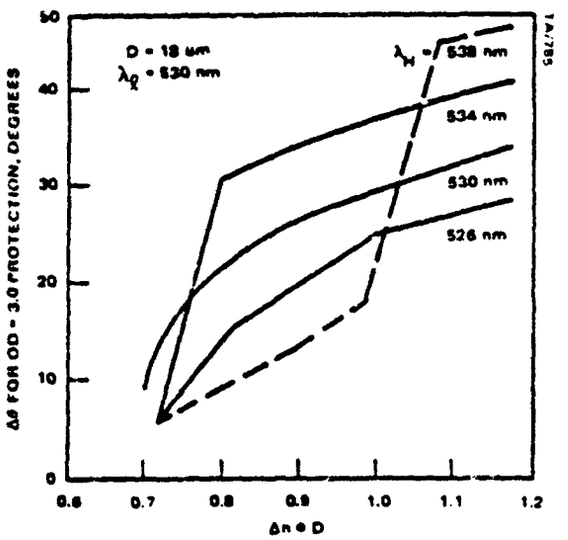

Figure 12. Analytical prediction of Δθ vs Δn·D for 18μ thick hologram

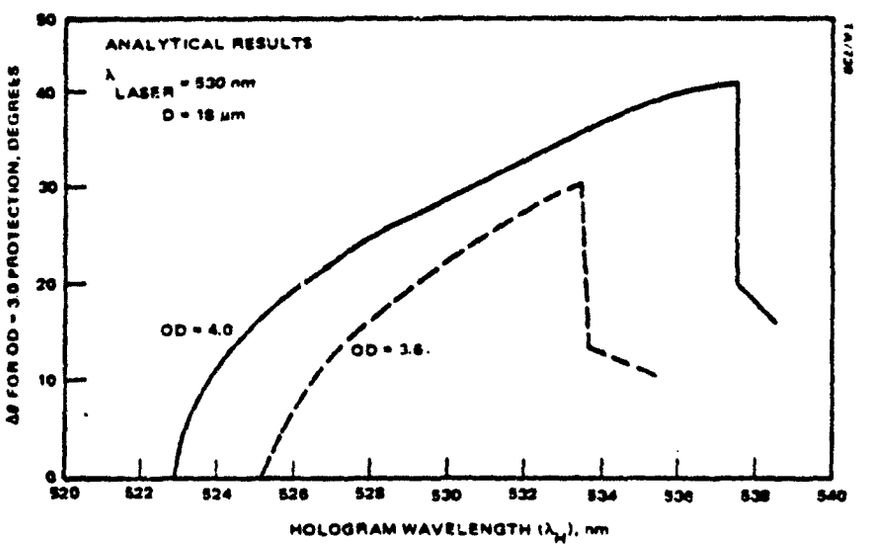

Figure 13. Angular protection (Δθ) varies as the hologram wavelength changes

2.0 THEORETICAL ANALYSIS

2.3 EXPERIMENTAL SAMPLES VERIFY THE THEORETICAL PREDICTIONS

The measured results from a number of experimental samples closely match the theoretical predictions. Therefore, the theoretical model can be used with good confidence as a design guideline for high efficiency holographic visor applications.

To verify the accuracy of the theoretical predictions against the actual hologram performances, a series of experimental samples were fabricated using a stable, yet simple optical set up shown in the Appendix, Figure A-15. The recorded hologram fringes were parallel to the subtrate surface ($\theta = 0$). The samples were then measured using a Cary Model 217 Spectrometer for efficiency vs θ. Photopic transmission was measured using a Standard Illumination (100ft-L) as the source and a Photo Research Pritchard Model 1980 "A" photometer as the detector. Glass substrates were used as a reference for all measurements, so the data represent the actual hologram performances alone, not including surface reflection by the substrate.

A typical sample #27 was measured and found to have peak efficiency of 99.99% (optical density OD = 4.0) at wavelength $\lambda_H = 529$ nm (Figure 14). As shown in Figure 15, the measured angular protection ($\Delta\theta$) is 26° at 528 nm and 35.5° at 523 nm for OD = 3.0 protection. The efficiency drops off very rapidly outside the angular range.

The variation of $\Delta\theta$ as a function of the wavelength of the incident radiation is shown in Figure 16. The solid line is the measured value of $\Delta\theta$ vs. λ. The dotted line in Figure 16 represents the calculated values based on the measured physical parameters of the hologram: gelatin thickness 16.3 µm, the peak wavelength $\lambda_H = 529$ nm, and the peak efficiency OD = 3.8 or 99.98%. Figure 16 clearly indicates that the experimental results and theoretical calculation of $\Delta\theta$ are in close agreement within the error of angular accuracy.

The photopic transmission of the experimental samples was also measured. Measurements were taken from several holograms while they were being baked. The baking gradually lowers the peak wavelength λ_H of the holograms. The photopic transmission T is the lowest when the hologram reflects most efficiently around 560 nm, which is the peak of human eye response. The curves in Figure 17 show the theoretical calculated value. The Differences between the experimental data points and the calculated values are less than 2%.

As the results of the study and experimental samples verify, there are two observations important to visor fabrication.

1) The experimental results confirm the analytical predictions on hologram properties with efficiency up to OD = 4.5. It is reasonable to use the analytical results as trade-off guidelines for the design of the laser eye protection visor.
2) The state of the art in hologram processing is used in the fabrication of experimental holograms. Hologram efficiency of up to OD = 5.0 has been

achieved, and efficiency of OD = 4.0 has been consistently fabricated. Therefore, at this development stage, it is realistic to expect angular protection of 30 to 35 degrees and photopic transmission of about 80% for the protection of .53 μm laser radiation.

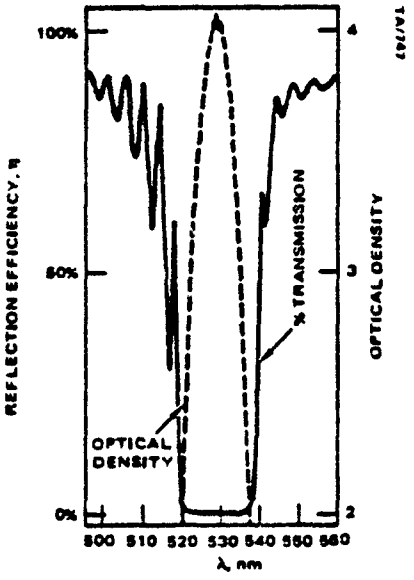

Figure 14. Efficiency vs wavelength for sample GM 27

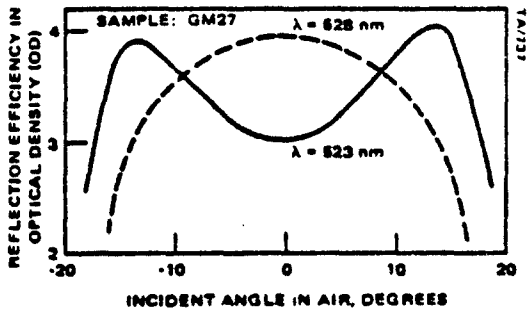

Figure 15. Angular dependence of efficiency at 528nm and 523nm

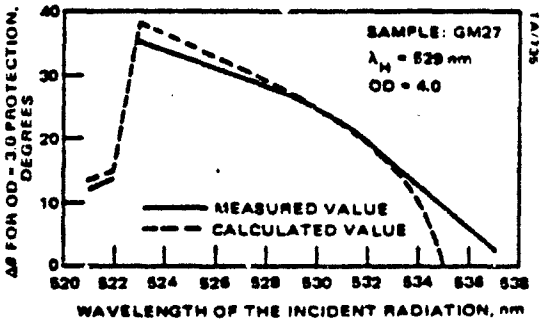

Figure 16. Protection angle (Δθ) vs wavelength of incident radiation

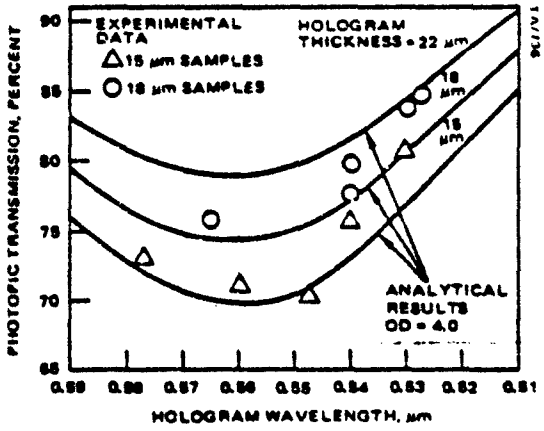

Figure 17. Photopic transmission holograms: comparison of analytical results and experimental data

2.0 THEORETICAL ANALYSIS

2.4 VISOR DESIGN: HUMAN FACTORS AND PROTECTION REQUIREMENTS

Human factors such as the location and the size of the eyes define the protection area for a visor design. As a design goal, the maximum transmission of laser radiation through the hologram and into the eye protection area is .1% or less.

An acceptable visor design should take into consideration not only hologram performance, but also human factors. The size and the location of the possible eye pupil area are the most important factors in determining the visor geometry and holographic design.

Interpupillary spacing varies among individuals (Figure 18). Extensive human factors data have been compiled and published in document MIL-STD-1472B. The relevant data are tabulated in Figure 18. To cover 5 to 95 percentile variation, the minumum eye size and eye spacing to be protected by the visor are derived as follows:

$$\text{Minimum eye size} = 1/2\ (\text{Max A} - \text{Min C}) = 1.455\text{"}\ (37\text{mm})$$

$$\text{Eye separation} = 1/2\ (\text{Max A} + \text{Min C}) = 2.535\text{"}\ (64.4\text{mm})$$

The minimum size of the possible eye position area is a 1.455" diameter region, centered at 1.27" from the midpoint of the area between the eyes. The dimension of the eye is smaller in the vertical direction (Figure 18). So the protection dimension required is correspondingly smaller as shown in Figure 20. There is no definite data from MIL-STD-1472B on this vertical dimension. For clarity of design, the position and the size of eye protection areas are sketched in Figures 19 and 20.

As far as the required radiation protection by the holographic visor, no extensive study was done in this contract. It is estimated that OD = 3.0 protection is very useful for applications such as rejection against target designators, range finders, and low energy blinding weaponry. Therefore, rejection efficiency of OD = 3.0 (99.9%) is used as the design goal for this contract.

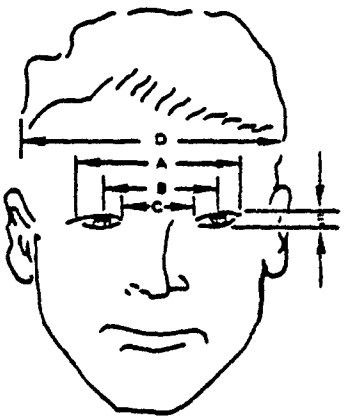

AVIATOR

	5%	95%
A	3.31"	3.98"
B	2.10"	2.75"
C	1.08"	1.50"
D	5.17"	5.98"

Figure 18. Interpupillary spacing data from MIL-STD-1472B

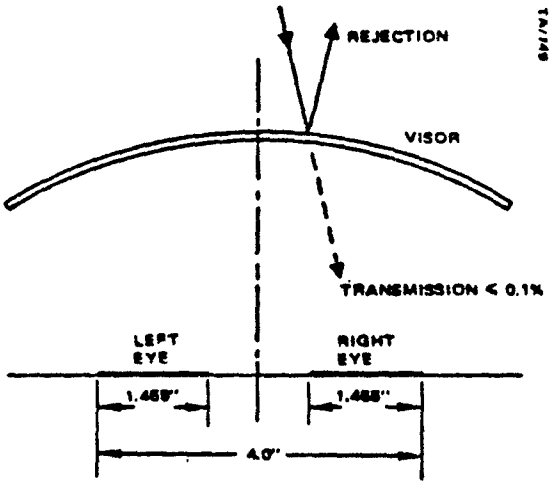

Figure 19. Horizontal dimension of the eye area and eye position

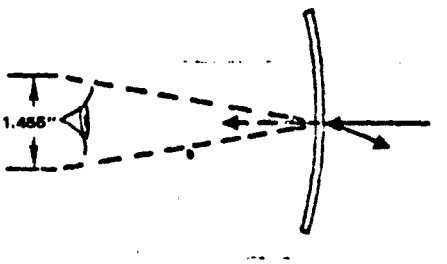

Figure 20. Vertical dimension of the eye area

2.0 THEORETICAL ANALYSIS

2.5 EFFECTIVE HOLOGRAPHIC VISOR DESIGN REQUIRES TWO HOLOGRAMS

Based on human factors and theoretical analysis, two holograms are needed to achieve adequate angular protection for two eyes. The protection system can be in the form of a visor or a goggle.

The angular protection required to protect the eye size determined in Section 2.4 is a function of the visor-eye distance d. It is desirable to keep the visor-eye distance to a reasonable range so that the visor does not protrude out to interfere with the visor user performing other tasks. Both the analytical and experimental results indicated that a single high efficiency hologram of OD = 4.0 can achieve $\Delta\theta$ of 34°-36°. For this angular protection, the visor distance must be 6.2" or longer to adequately protect a 4" area covering both eyes. To reduce the visor distance to about 3" requires $\Delta\theta$ to be 67° or larger, which is theoretically impossible to obtain from even a perfect single hologram. Therefore, two holograms are needed to provide protection for both eyes. There are two design approaches for two hologram protection: visor design and goggle design.

1) Visor Form

As shown in Figure 21, the visor consists of two separate holograms laminated together, one to protect the right eye and one to protect the left eye. Considering the eye sizes and practical limitation of angular protection at 30° by a single hologram, a specific visor geometry is designed as follows:

Visor distance d = 75mm
Visor curvature R = 146mm

With this geometry, the required $\Delta\theta$ protection at different points of the visor are calculated and shown in Figure 22 for both eyes. The maximum requirement is 29.8° which has been achieved experimentally for a single hologram. The hologram for protecting each eye requires the same $\Delta\theta$, oriented in opposite directions. It is the goal of this contract to fabricate a mock-up visor of this visor design.

2) Goggle Form

The goggle type design shown in Figure 23 consists of two separate eye pieces. Each eye piece is again formed with two holograms; one protects half of the eye area and the other protects the other half of the eye area. If each hologram provides a 30° protection angle, two holograms properly oriented can provide 60° of protection. This reduces the visor distance d to about 33mm (1.3").

Because of the short visor distance, the junction between the two eye pieces does not distort the imagery, and thus does not degrade normal vision. This design may be useful to shipboard personnel who have to move around to perform their tasks.

It was not within the scope of this contract to fabricate a full goggle for evaluation, but only to prove the design concept. For this purpose a "double-skew" hologram, consisting of two holograms laminated together, was constructed and experimentally evaluated.

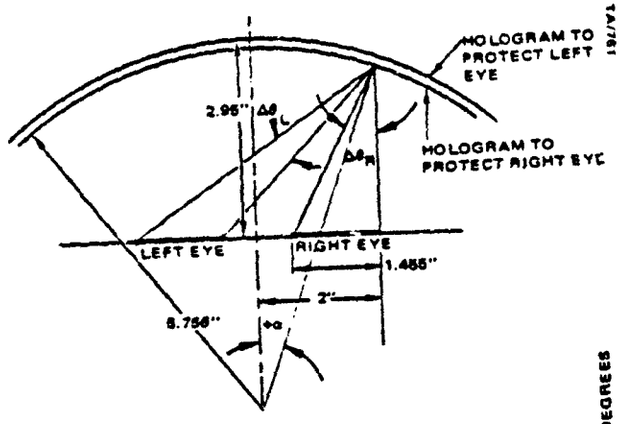

Figure 21. Visor design using two holograms

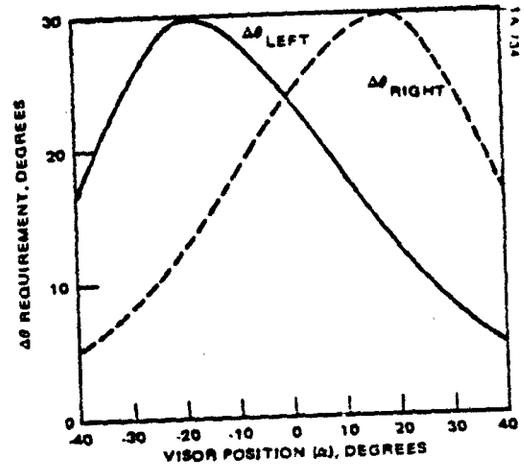

Figure 22. Δθ requirement for the visor design shown in Figure 21

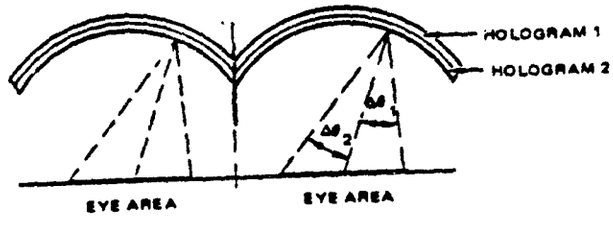

Figure 23. Double hologram goggle design

3.0 LASER VISOR MOCK-UP

3.1 VISOR MOCK-UP CONSISTS OF FOUR DOUBLE HOLOGRAM SEGMENTS

The mock-up is divided into 4 equal segments to reduce the complexity and the cost of the hologram exposure optics. Each segment consists of two holograms exposed separately using a corresponding pair of cover and mirror lenses.

To establish the feasibility and to evaluate the visor design described in Section 2.5, a strip of visor hologram is fabricated for full horizontal viewing and limited vertical viewing. The visor strip or mock-up is further divided into four equal segments to reduce the complexity and the cost of hologram exposure optics. Figure 24 shows that the visor mock-up consists of 4 pieces of 2" x 2" spherical shape visor segments. The visor segments are identified as A, B, C, & D for easy reference. Each segment is of course a lamination of two holograms. The holograms are labeled as I, I', II, II', etc.

The primed and unprimed holograms (I, I', etc) are identical holograms which are oriented oppositely in the visor to protect either the right or left eye. Therefore, the task of visor fabrication is reduced to the fabrication of 4 holograms I, II, III, IV, as shown in Figure 25. As shown, these holograms are in the geometry to protect the right eye.

Each hologram is designed to provide protection against laser radiation aiming toward the center of the eye F, as shown in Figure 26. The holographic fringes are oriented perpendicular to the ray direction in the recording medium. The fringes are generally slanted with respect to the surface of the substrate. This orientation provides the widest angular range centered around the middle of eye protection area.

To generate the design fringes, two possible recording optical systems are considered. In the first system as shown in Figure 27, the exposure light beam originates from the center of the eye position F. The exposure beam, after passing through the hologram substrate, is reflected back by a mirror M to its incident direction. The exposure beam and the reflected beam produce interference fringes oriented at the proper direction. The drawback of this approach is the multiple reflection between hologram substrates and the mirror surfaces. The reflection could produce ghost images and reduce the overall efficiency. Because of the multiple reflections, this approach was abandoned. The second approach is used for this contract.

The second approach shown in Figure 28 is again designed to produce holograms described in Figure 26. Using two solid glass block lenses, the exposure light originates at Point G which is not the center of eye area, but is the intercept of light rays inside the hologram medium (Figure 26).

The point G is also the center of curvature of the mirror surface and the outer surface of the cover lens. The incoming exposure beam diverges from G, enters into the glass lens unrefracted, and is retroreflected by the mirror lens. The thicknesses of both lenses are determined by the minimum

glass thickness that can be easily fabricated by the optical vendor. The spaces between the lenses and the hologram substrate are filled with index matching fluid to minimize the interface reflections. Each of the four visor segments has a different focal point and orientation. Therefore, the visor exposures require 4 sets of cover lenses and mirror lenses. Figures A-1 through A-4 show the detailed optical layout of the four lens sets. The substrate is .075" thick and 3.1" in diameter. After exposure and processing, the substrates will be laminated and cut to 2" x 2-1/8" segments to be assembled into a visor for lab tests.

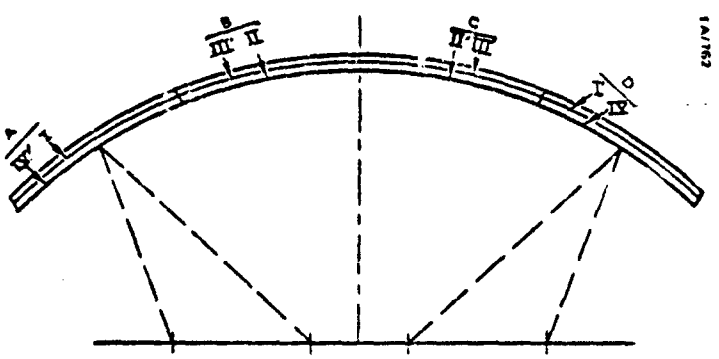

Figure 24. Visor mockup consists of four segments (each segment includes two holograms)

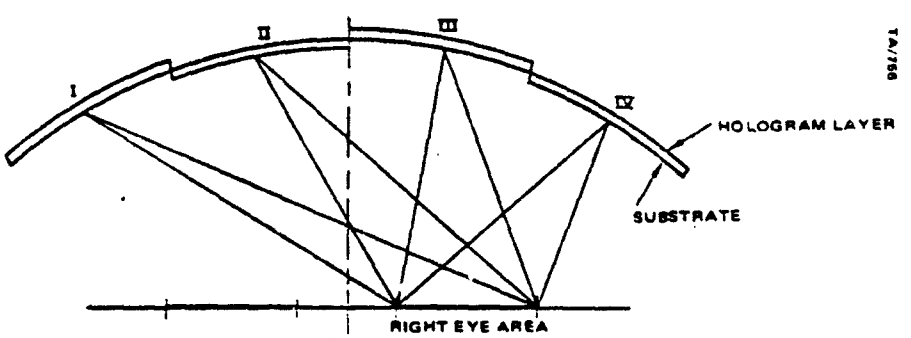

Figure 25. Holograms required for visor mockup

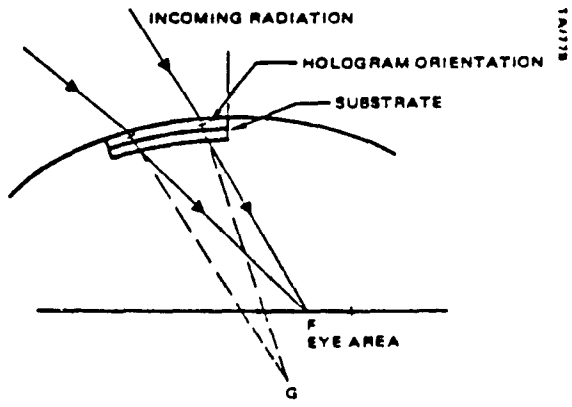

Figure 26. Hologram fringe orientation and beam direction in the hologram

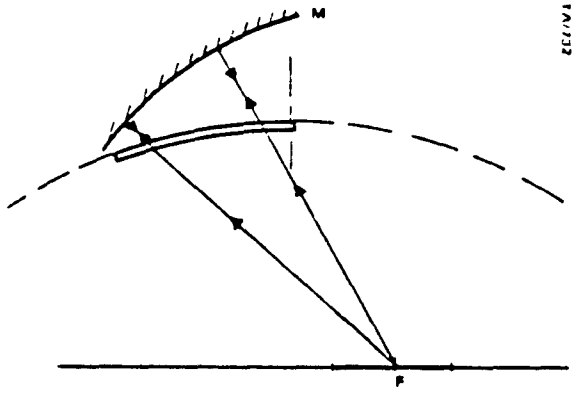

Figure 27. Exposure optics for visor hologram: Option I

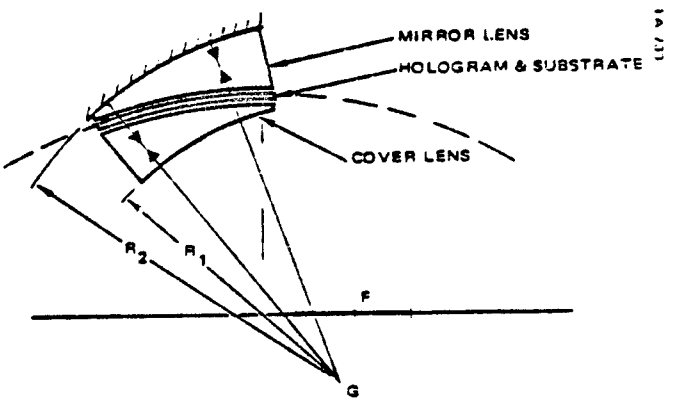

Figure 28. Exposure optics for visor hologram: Option II

3.0 LASER VISOR MOCK-UP

3.2 EXPOSURE SYSTEM PROVIDES HIGH EXPOSURE ENERGY AND HIGH STABILITY

An extremely stable exposure set up is essential for a high efficiency hologram. The stability is continuously monitored by an interferometric sytem. High exposure energy is also used for a high efficiency hologram.

To record high efficiency holograms as designed in Section 3.1, there are two key factors to be considered: high exposure energy and high mechanical stability during the exposure process. An unstable exposure system increases the background exposure and makes the index modulation (Δn) smaller. High exposure energy is needed to achieve Δn as high as possible.

Figure 29 shows the detailed design of the holding fixture for a pair of exposure optical lenses, cover lens and mirror lens. The holding fixture is designed to hold all 4 sets of exposure lenses for the 4 visor segments. In this set up, the substrate is firmly attached to the mirror lens so that both the substrate and the mirror lens experience the same type of vibration. When the substrate and mirror move in step, then the movement does not affect the holographic fringe formation. The substrate is placed horizontally in the fixture so that the index matching fluid can stay in the interface region to minimize the interface reflection. The mirror surfaces were coated with a silver coating of 95% reflectivity. The first surface of the cover lens is coated with an anti-reflective coating with reflectivity less than .2% at the exposure wavelength of 5145Å. Orientation markers are scribed on the substrate side of the lens cover. The marks are out of the visor hologram area and are used to identify the proper hologram orientation during lamination and final assembly.

Figure 30 shows the overall exposure optical system. Each segment requires a different focal point to substrate distance and also a different orientation angle as explained in Figures A-1 through A-4. Therefore the spatial filter is located at a different position for each segment. The mirror M is also tilted at slightly different angles for each segment.

To avoid any stray exposure light hitting the edge of the exposure lenses, careful masking of the aperture is required for each exposure. The masks are positioned at the conjugate image plane of the substrate so that the hologram formation by edge diffraction from the mask is kept to a minimum.

A Michelson type interferometer is also set up to monitor the stability of the exposure apparatus. For a typical stability scan during the exposure period, stability better than $\frac{\lambda}{15}$ is achieved in the 1-1/2 minute exposure period.

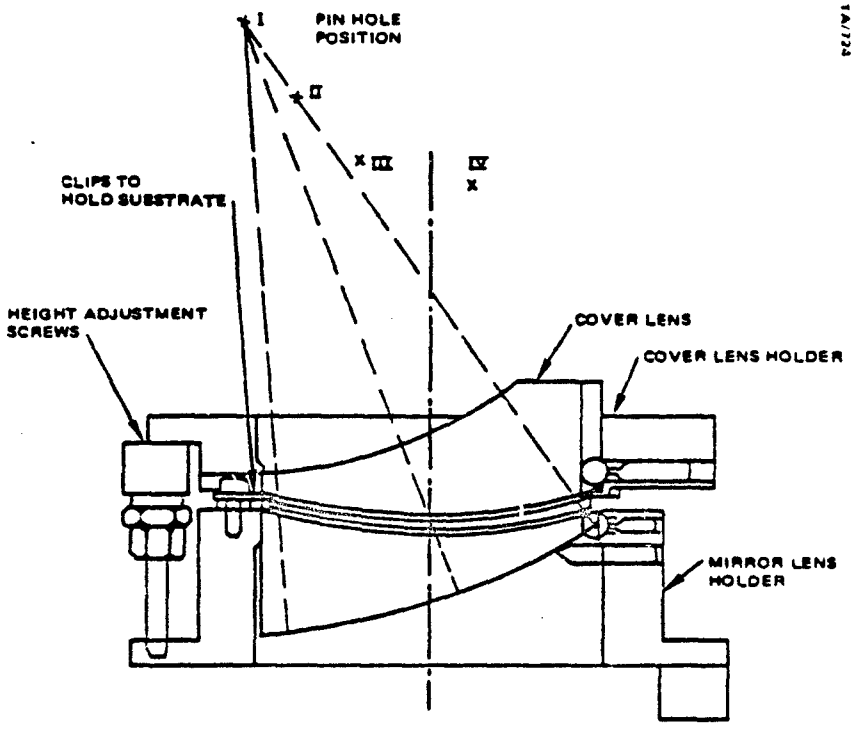

Figure 29. Mechanical fixture for the exposure optics

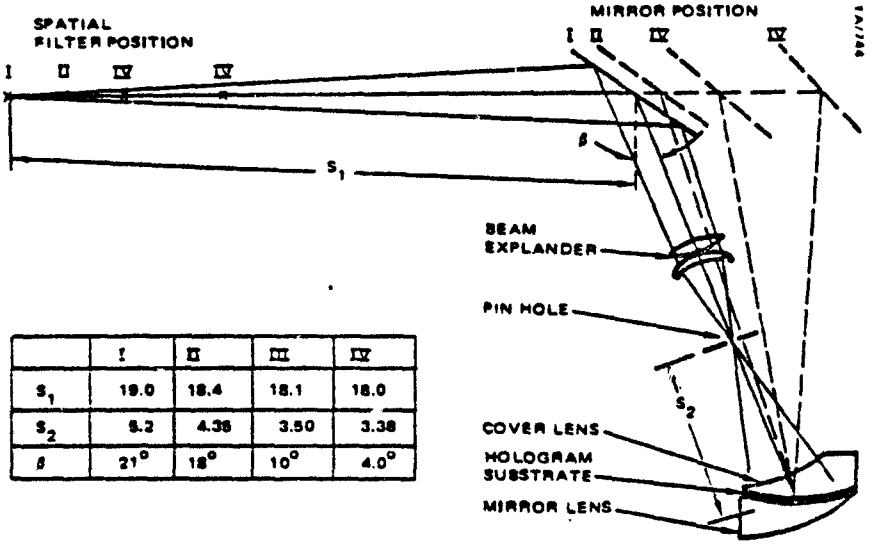

	I	II	III	IV
S_1	19.0	18.4	18.1	18.0
S_2	5.2	4.38	3.50	3.38
β	21°	18°	10°	4.0°

Figure 30. Overall optical setup for the exposure of four visor holograms

3.0 LASER VISOR MOCK-UP

3.3 PROCESSING OF VISOR HOLOGRAMS

Besides stable exposure, there are several critical factors for high efficiency hologram fabrication. The critical factors include choice of recording materials and precisely controlled coating and processing steps.

In the fabrication of high efficiency holograms, there are a number of critical factors. Exposure stability is one factor which was discussed in Section 3.2. For the interest of a complete discussion, the other factors include choice of recording materials, coating process, developing process, and sealing and baking processes.

1) Recording Material - It is widely recognized that dichromated gelatin can provide the highest Δn and lowest scattering loss among all of the available photosensitive recording materials. The drawback is that it is difficult to obtain consistently reproducible results unless precisely controlled processes are followed. Fortunately, the needed processes and controls have been previously developed at Hughes. For the laser eye protection visor, which requires extremely high efficiency holograms, it appears that dichromated gelatin is the only acceptable material at this time.

2) Coating Process - The temperature and humidity level during the coating and gel drying can significantly influence the coating photosensitivity. The thickness of the coating is also an important factor affecting the uniformity of the hologram efficiency across the format. All these parameters have been tightly controlled during the preparation of the visor coatings. Figure 31 shows the processing equipment used.

3) Exposure Energy Level - The required energy for high efficiency varies if the coating is prepared at different conditions. To identify the desired level, a series of tests was carried out to determine experimentally the exposure energy needed.

4) Developing & Baking Process - All samples were developed under controlled temperature baths and dryed under a dry nitrogen environment to prevent the hologram from contacting the humidity. A slight amount of humidity may significantly decrease the peak of efficiency of the hologram. The processed samples then were placed in an N_2 atmosphere oven to shrink the gelatin film and obtain the design wavelength.

All the above mentioned conditions were fine tuned during the fabrication of the experimental samples described in Section 2.3. Holograms with 99.99% efficiency (OD = 4.0) were obtained consistently. These conditions were then used to fabricate the visor holograms as shown in Figure 32.

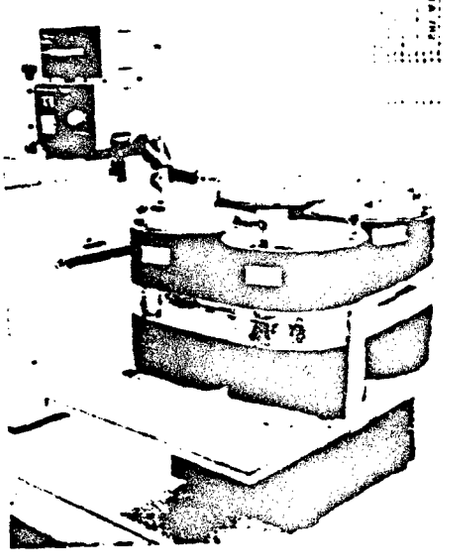

Figure 31. LEP processor

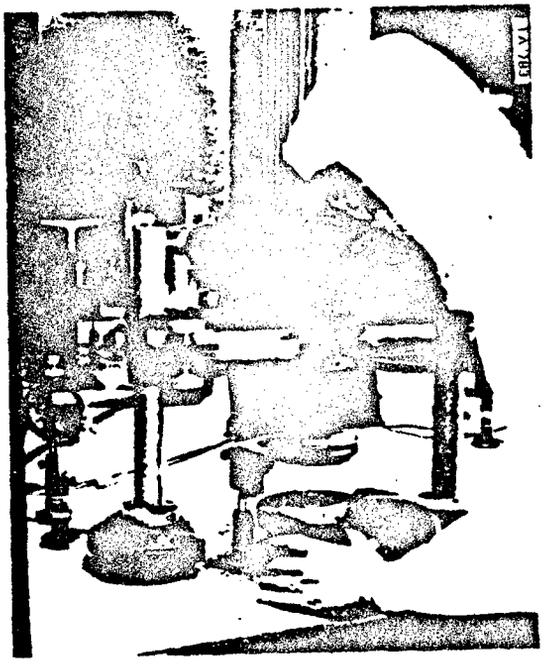

Figure 32. Exposure apparatus for visor holograms

3.0 VISOR MOCK-UP

3.4 THE MOCK-UP ACHIEVES HIGH REJECTION EFFICIENCY AND EXCELLENT SEE-THROUGH

The mock-up visor has demonstrated the feasibility of fabricating high efficiency holograms to protect designated eye areas. Some of the difficulties of the fabrication are also useful as guidelines for future design.

Two pieces each of the four visor holograms were exposed and processed. The matching holograms were then sealed together and cut into size (2" width x 2-1/8" height). The laminated segments were assembled into a visor holder to form a mock-up visor as shown in Figure 33. The mock-up may be worn to demonstrate the see-through and the user acceptance of the holographic visor.

Extensive measurements were performed on the visor segments. To illustrate the essential properties, the results of visor segment "A" are summarized in Figures 34-37. The details of each figure will be explained. The results of the other segments are comparable and are summarized in the appendix in Figures A-5 through A-14.

For visor segment A, peak efficiency of OD = 4.8 (99.998%) at 542 nm and incident angle $\theta = 21^{o}$ were measured. As shown in Figure 34, at an incident angle $\theta = 33^{o}$, the peak efficiency is OD = 4.75 at 530 nm. For incident radiation at 544 nm, Figure 34 shows that the hologram provides $\Delta\theta = 39.5^{o}$ of OD = 3.0 protection, with peak protection efficiency at OD = 4.75. For incident radiation at 530 nm, the hologram provides $\Delta\theta = 12^{o}$ at a different angular direction. The unsymmetrical shape in efficiency vs. θ is due to the interaction of two laminated holograms.

The angular protection vs. the actual eye position is plotted in Figure 35. It indicates that the measured protection range is more than adequate to cover the entire left eye if incident beam wavelength is 544 nm. The protection angle at 530 nm covers all the intended right eye position. The fact that there are two different wavelengths (544 nm and 530 nm) for the visor segment is due to the different wavelengths of the two holograms (I, IV') sealed together. We will discuss this further in the next section.

Figure 36 illustrates the changes of wavelength of peak efficiency with respect to the incident angle at the center portion of the visor segment "A". One hologram (IV') is peaked at 556 nm with fringe slant angle of about 4^{o}. The other hologram (I) is peaked at 537 nm with slant angle at 32^{o}. These measured slant angles correspond to the optical design angles described in Section 3.1. The difficulty of achieving precise wavelength match over the format and methods for improving the match are discussed in Section 3.5.

Figure 36 also relates the photopic transmission (T) with the viewing angle. See-through level is 63-71% for the right eye and 67.5-84% for the left eye. The lowest T is 63%, which is lower than expected from theoretical analysis of a double hologram. It is primarily due to the mismatch of the peak wavelengths of the two holograms. Each hologram reflects efficiently in one spectral band. The visor segment acts as a broadband reflector (as shown in Figure 37), which minimizes the see-through level. A properly matched visor segment will have higher photopic transmission.

The wavelength uniformity (Figure 37) shows that the peak wavlength at various positions on the hologram varies up to 22 nm.

The results for visor segments B, C, D are comparable to the results for segment A. However, distant objects seen through segment B and C appear fuzzy with some loss in resolution. Close examination indicates that one of the sealed holograms (III) is fuzzy and distorts transmitted images. The exact cause is not clear. No such distortions were noted in other holograms (I, II, & IV). We speculate that the processing temperature may have been near the cracking range of the hologram medium for III, so that excessive scattering and fringe plane distortion cause lower resolution and a fuzzy appearance. Since it is not universal, but occurs only in hologram III, the problem can be eliminated with tighter process control as described in Section 3.3.

To summarize the performance of the mock-up visor, it definitely demonstrates that high efficiency visor holograms can be fabricated to protect the designed eye area with excellent see-through. However, improvements are needed in the area of developing process as well as wavelength monitoring. This visor study also raises some engineering pitfalls to be avoided in future designs. These pitfalls will be discussed fully in the next section.

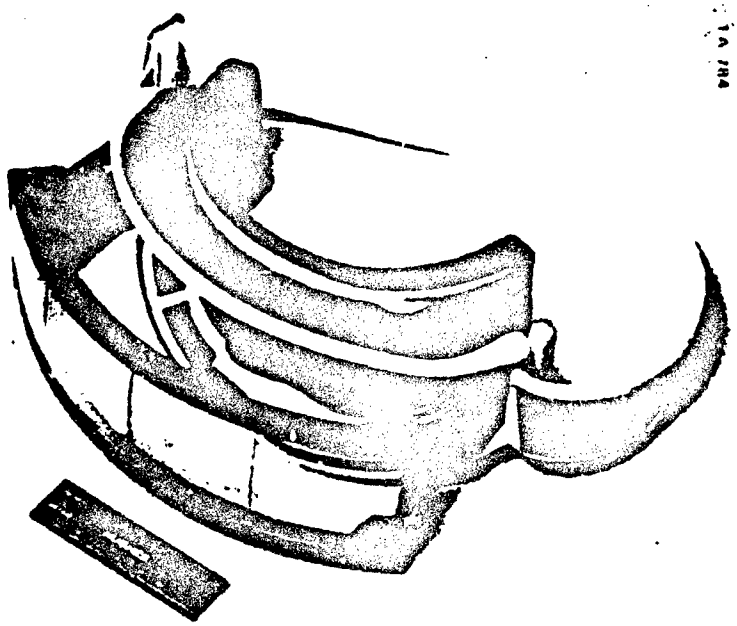

Figure 33. Holographic visor mock-up

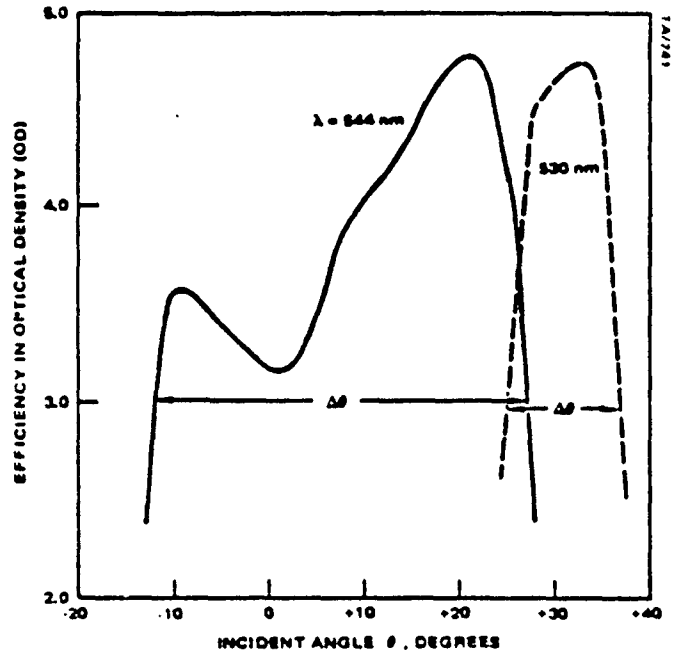

Figure 34. Hologram efficiency vs incident angle for visor segment "A"

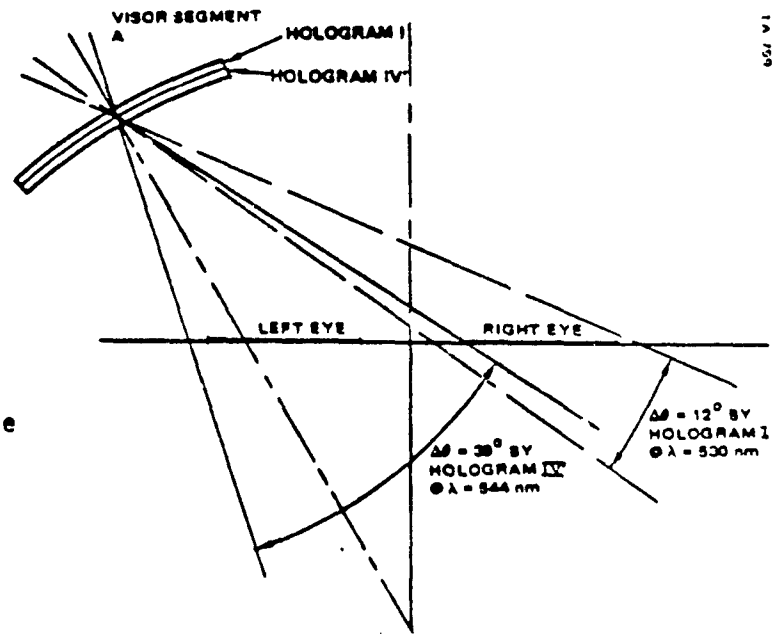

Figure 35. Protection angle at the center of visor segment "A" (protection is adequate for both eyes)

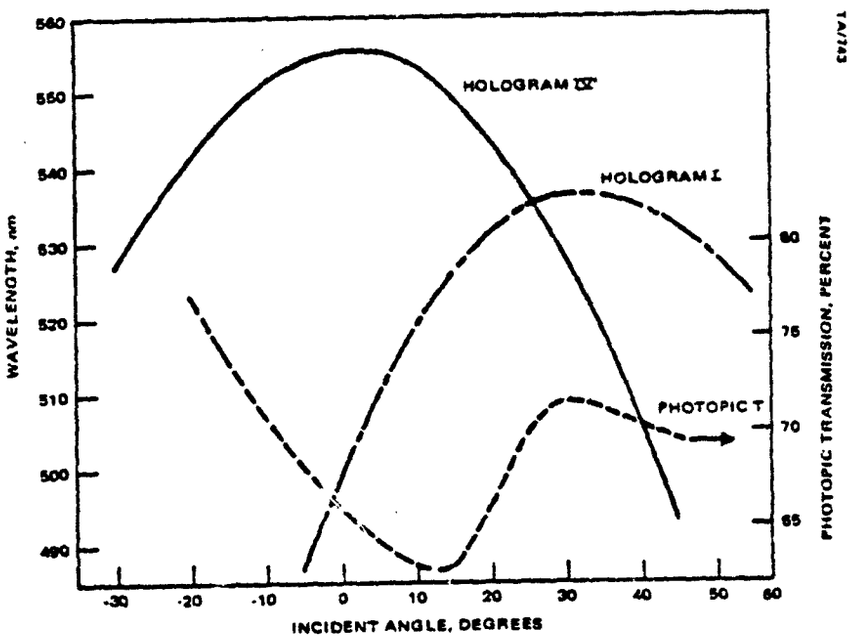

Figure 36. Peak wavelength and photopic transmission as a function of incident angle for visor segment "A"

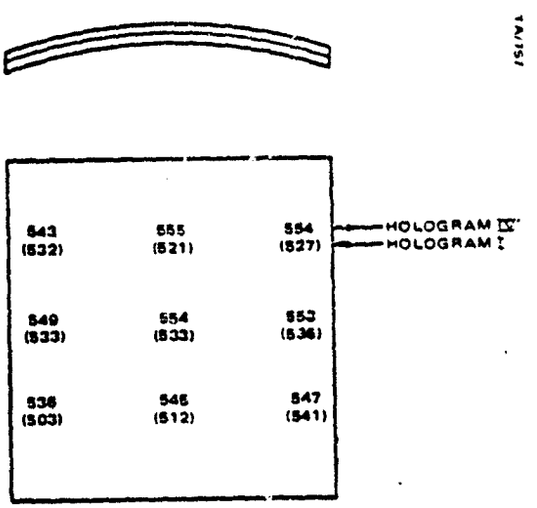

Figure 37. Hologram wavelength at various portions of the visor segment "A"

3.0 LASER VISOR MOCK-UP

3.5 PITFALLS OF THE SLANTED FRINGE HOLOGRAM

A hologram with slanted fringes has several shortcomings which require further development effort to overcome. The shortcomings include lower efficiency, poorer wavelength stability, and the existence of an extra diffraction spot due to the surface grating.

In the visor mock-up unit, efficiency as high as 99.99% was achieved. However, the efficiency across the visor varies from 99.99% to 99.7%, and the hologram wavelength varies up to 22 nm. Careful evaluation shows that the slant angle of the holographic fringes has a profound effect on the efficiency and the bake-down wavelength. Since the slant angle varies continuously across the visor under the present visor design, it is difficult to obtain uniformity.

A slant fringe hologram is schematically described in Figure 38. The fringe plane is not parallel to the substrate surface, but makes an angle ϕ. The slant angle may not be a problem in a low-efficiency hologram, but it causes a number of serious difficulties in fabricating a high efficiency hologram as in the case of the visor. Major problems include: lower efficiency, varied baking rate, and extra diffraction due to the thin surface grating.

1) Efficiency: It is suggested by Curran & Shankoff, that micron-voids are developed in the gel during the developing process. The region with many voids is the lower index region. The harder region that does not contain many voids is the higher index region. The voids are generated when the gel is swollen and then dehydrated by 2-propanol. The free movement of the hardened layer is essential to the swelling action, and therefore the creation of micro-voids.

In a slant angle hologram, experimental results indicate that the gel does not swell up as much as in the case for $\phi = 0$. We suggest that the hardened layers are anchored on the substrate surface which prevents the free expansion of the gel. Because of the restrictive swelling, fewer voids are generated, and lower Δn and efficiency result.

We have varied the processing techniques to successfully fabricate OD = 3.75, 10^{o} slanted holograms compared to OD = 3.0 before processing modifications. However further development effort is needed to consistenzly fabricate high efficiency slant angle holograms.

2) Baking Rate: Immediately after the developing, the hologram gel is in the swollen state. High temperature baking of the hologram is used to shrink the gel. As the gel shrinks, so does the fringe spacing Λ and the corresponding hologram wavelength λp. ($\lambda p = 2\Lambda n_o$, where n_o is the average index of refraction).

Because of the anchoring of the fringes on the substrate, the shrinking is strongly affected by the slant angle ϕ. We have found that the larger the slant angle, the faster the decrease of fringe spacing. This is the reason that it is difficult to obtain the same wavelength protection across the visor on the present mock-up in which the slant angle ϕ varies

from 0^0 to 23^0. In order to improve wavelength uniformity, either the processing must be varied across the surface or the design must be changed to reduce the differential slant angle.

3) Diffraction By Thin Surface Hologram.

It is observed that an extra diffraction spot was generated when the laser beam went through the slanted hologram. No such diffraction was observed from a zero slant ($\phi = 0^0$) hologram.

Results of evaluations indicate that the location of the diffraction spot is related to the surface spacing (d) of the slanted fringes. Angular measurements further indicate that the diffraction is primarily due to the thin surface grating formed by the slanted fringes on the interface. Figure 39 illustrates that equivalent thin hologram. The diffraction angle θ_r and the incident angle θ_i, are related by the grating equation:

$$\sin \theta_i + \sin \theta_r = \frac{\sin \phi \cdot \lambda o}{\Lambda}$$

At certain areas of the visor mockup, Λ, ϕ, θ, are related in such a way that the extra diffraction may enter into the eye area. At this stage, the diffraction efficiency is estimated to be about .2 to .3% of the incident energy. In the design of future visors, this diffraction spot will either be eliminated or directed away from the eyes.

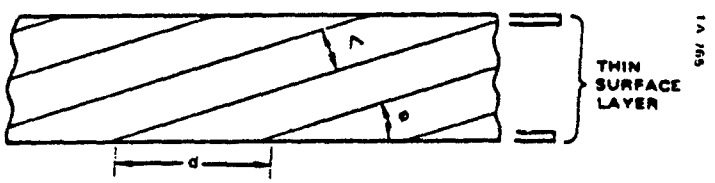

Figure 38. Hologram with slant fringes at angle ϕ

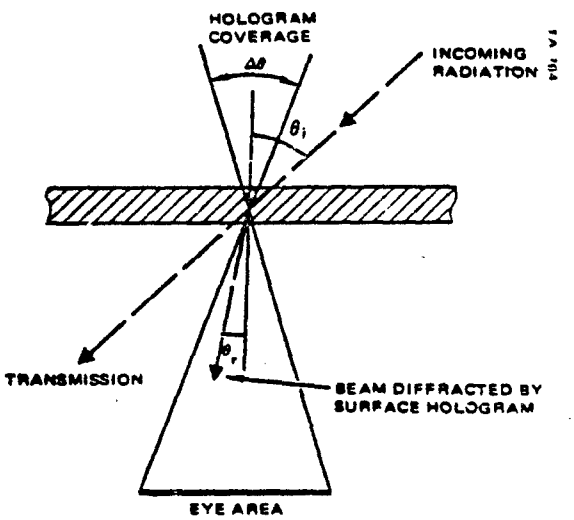

Figure 39. Light diffracted by the thin surface layer on a slanted fringe hologram

4.0 DOUBLE SKEW HOLOGRAMS

4.1 UNIQUE DESIGN PROVIDES GREATER ANGULAR COVERAGE

Using a special double hologram design, two holograms with skewed fringes can be sealed together to provide approximately twice the angular protection of either hologram alone. Therefore the distance between the eyes and a goggle or visor can be reduced.

A single hologram can only provide about 30° of angular coverage which would provide adequate protection to one eye at a distance of 73.3 mm from the eye. Because of the increased angular coverage required for a laser eye protection goggle closer to the eye, a single hologram cannot provide adequate protection even to one eye. The solution, as indicated in the chart below, is to use two holograms sealed together to decrease the distance and provide the extended angular coverage.

Using a simple technique, a hologram can be fabricated so that the fringes in the gelatin are at an angle to the gelatin plane instead of parallel to it. The resultant angular coverage is shifted a few degrees away from the normal to the plate as shown in Figure 40. Two such holograms can be sealed together to make a double skew hologram. The two slanted fringe holograms are oriented so that the peak efficiencies are on either side of 0° incidence. The double-skew hologram that results provides approximately twice the angular coverage of a single hologram at the same distance.

Average Coverage Required ($\Delta\theta$)	Visor Distance (mm) Single Hologram	Visor Distance (mm) Double-Skew Hologram
25°	88.2	42.1
30°	73.3	34.0
35°	62.9	28.0
40°	53.9	23.4

A theoretical calculation of the angular coverage of a double skew hologram is shown in Figure 41. In this calculation holograms R1 and R2 have an angular coverage of slightly less than 30° each. The combined coverage for the two sealed together is almost 60°. As illustrated in Figure 42, a double skew hologram could be used in an eye protection goggle configuration. The maximum distance of the goggle from the eye is 1.25 inches. For the right eye, hologram R1 protects the angles to the left side of zero degrees, and R2 protects the angles to the right side. A double skew hologram of similar construction would provide protection for the left eye.

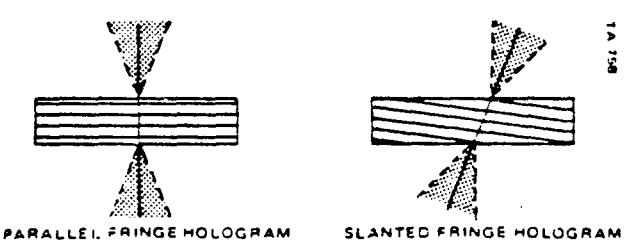

Figure 40. Angular coverage shifts away from normal for slanted fringes

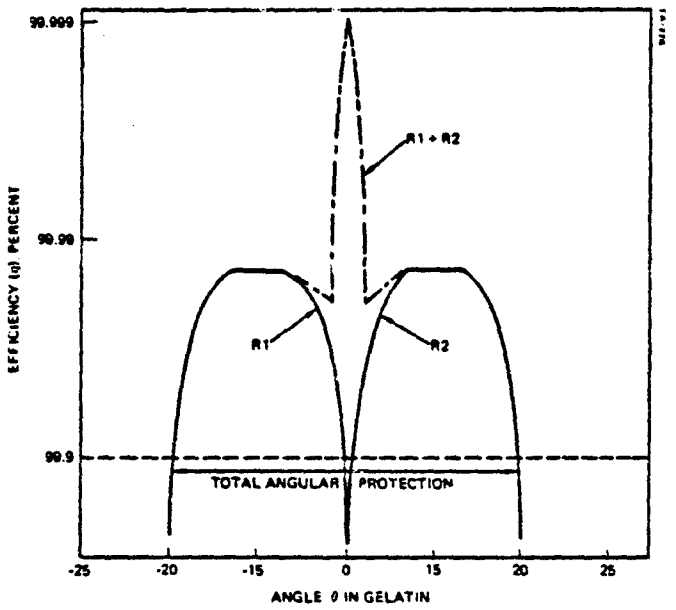

Figure 41. Theoretical increase in angular protection for double-skew holograms

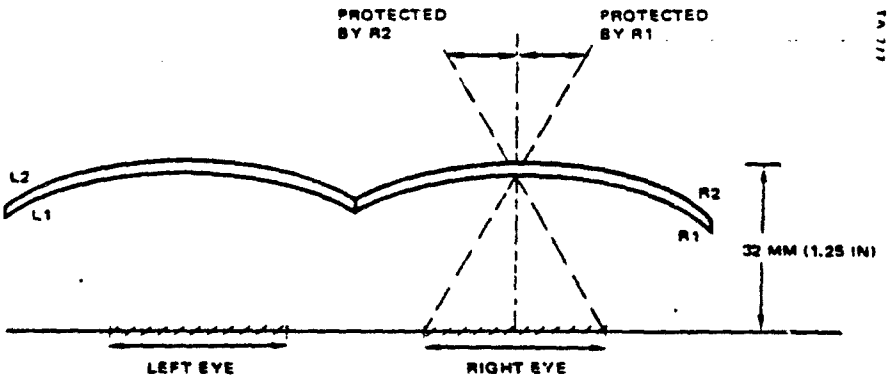

Figure 42. Possible goggle configuration using slanted fringe holograms

4.0 DOUBLE SKEW HOLOGRAMS

4.2 FABRICATION OF HOLOGRAMS WITH SLANTED FRINGES

The exposure system for slanted fringe holograms is typical of reflection holograms except for the addition of a wedge prism to provide the desired slant angle. However, the processing and sealing of these holograms requires special techniques.

For the experimental double skew holograms a 10^{o} angle was chosen for the fringe slant, so a 10^{o} wedge prism was used to produce the angled fringes in the gelatin substrate. The exposure system is sketched in Figure 43. The incident angle can be varied to tailor the fringe spacing for a peak efficiency at a chosen wavelength.

To fabricate a double skew hologram, two slanted fringe holograms are exposed identically. Then the holograms are sealed together with opposite orientations so that the peak angular protection of the holograms is shifted to either side of 0^{o}. Figure 44 illustrates how two holograms can be sealed to form a double-skew hologram with increased angular coverage.

In slanted fringe holograms, the fringes contact the surface of the gelatin. This anchoring of the fringes to the gelatin surface causes a restriction in the swelling and shrinking of the gelatin during processing. The result is that slanted fringe holograms have lower efficiencies than holograms with fringes parallel to the gelatin plane which were processed identically. By varying the coating and processing parameters, reflection efficiencies of greater than 99.9% have been achieved. Further refinements in the coating and processing techniques are necessary to achieve high efficiency results consistently.

Before sealing two slanted fringe holograms together, careful measurements in a 0% relative humidity environment are required to match the peak wavelengths. During the sealing process even slight residual moisture in the sealant can cause different shifts in the peak wavelengths of the two holograms. Since the slant angle is the same throughout the hologram, the bakedown rate is a constant across the format.

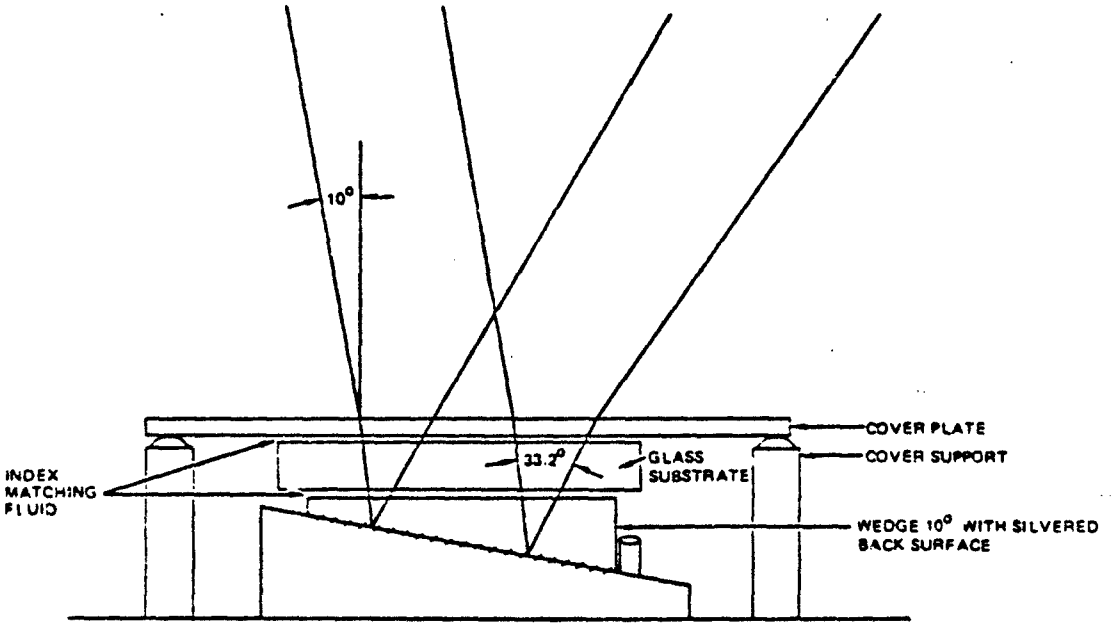

Figure 43. Skew hologram setup: 10^{0} wedge

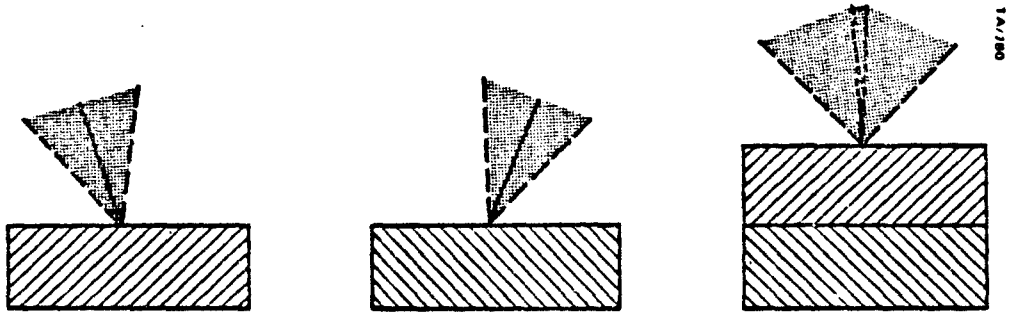

Figure 44. Improved angular coverage for double-skew hologram

4.0 DOUBLE SKEW HOLOGRAMS

4.3 EXPERIMENTS PROVE DOUBLE SKEW HOLOGRAMS WORK

Measurements of the reflection efficiency versus angle show that the double skew hologram method does extend the angular coverage.

Double skew holograms produced thus far achieve reflection efficiency of 99.86% (OD 2.84) for an angular coverage of up to 66.5°. The variation of the efficiency with angle for a typical double skew hologram is shown in Figure 45. The multiple peaks are due to the combination of the angularly dependent efficiencies of the two holograms. The dip below OD 3 at 0° is the result of a slight mismatch in the peak wavelength of the two slanted fringe holograms. The angular coverage shown is provided at 531 nm. The Cary scans of efficiency versus wavelength, corresponding to several angles, are shown in Figure 46. These scans illustrate that the bandwidth of coverage varies greatly with angle. Likewise, the angular coverage varies greatly with the wavelength. Great care must be taken in choosing the two holograms which together will provide the necessary angular coverage and bandwidth at the desired wavelength.

The angular coverage of a single 10° hologram is shown in Figure 47. This hologram is particularly efficient with almost 40° of angular coverage at 539.3 nm. The minimum see-through transmission for this plate is 82%. As would be expected, the photopic transmission of a double skew hologram is lower than for a single hologram. For the double skew hologram above, the photopic transmission is 73%. For protection at wavelengths not so near the peak sensitivity of the eye, the photopic transmission would be much higher.

When comparing the theoretical and experimental values of the photopic transmission for both single and double skew holograms, the experimental results duplicate the form of the theoretical results, but at a slightly lower transmission. The difference is due to scattering losses in the gelatin which can be significantly reduced with refinements in the processing techniques.

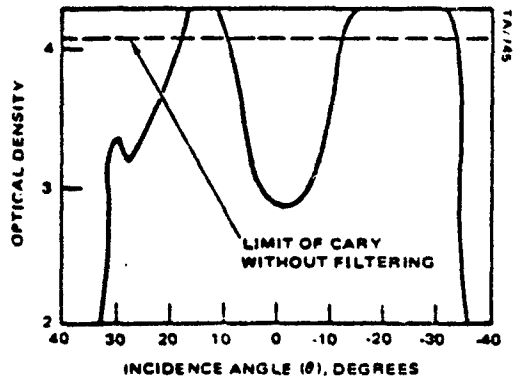

Figure 45. Angular dependence of efficiency at λ = 531nm

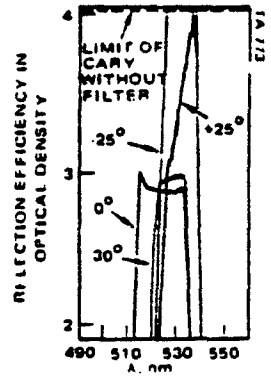

Figure 46. Efficiency of a single hologram measured at three different angles

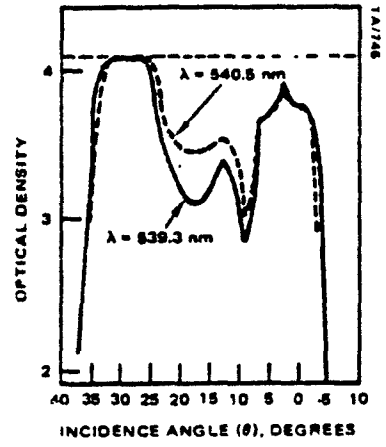

Figure 47. Angular dependence of efficiency for single 10^{0} hologram

5.0 1.06 μm HOLOGRAMS

5.1 EXPOSURE AT 5145 Å FOR PROTECTION AT 1.06 μm

The spectral sensitivity of dichromated gelatin does not extend into the infrared wavelengths. Therefore, the holograms must be exposed in a special configuration at 5145 Å to give a peak playback wavelength of 1.06 μm.

There is a growing need for laser eye protection at infrared wavelengths. The 1.06 μm laser wavelength is a popular choice for range finders, laser target designators, guidance systems, and other military applications. It is chosen because it is not visible to the eye and yet is still close enough to the visible to use conventional optics. These two reasons make 1.06 μm lasers even more hazardous than visible lasers.

As shown in Figure 48, dichromated gelatin is not sensitive to light in the infrared wavelengths; therefore, the current technology must be extended to fabricate efficient 1.06 μm holograms. Three techniques which make the fabrication of 1.06 μm holograms possible are:

1) dye sensitization to extend the gelatin response to longer wavelengths
2) swelling of the gelatin to increase the fringe spacing
3) modified construction geometry to yield 1.06 μm playback.

For this program the modified construction geometry was chosen as the best method to demonstrate the feasbility of 1.06 μm eye protection.

To expose 1.06 μm holograms with laser radiation at 5145 Å, the exposure geometry must be designed such that the exposure angles are greater than the playback angles. The fringe spacing, Λ, is a function of both the wavelengtn and the angle, θ, between the construction beams.

$$\Lambda = \frac{\lambda}{2n \cos \frac{\theta}{2}}$$

A hologram exposed at 5145 Å with $\theta = 122^{\circ}$ has a fringe spacing of 3490 Å which provides peak playback efficiency at 1.06 μm for near normal incidence. Figure 49 illustrates the construction and playback geometry for a 1.06 μm hologram.

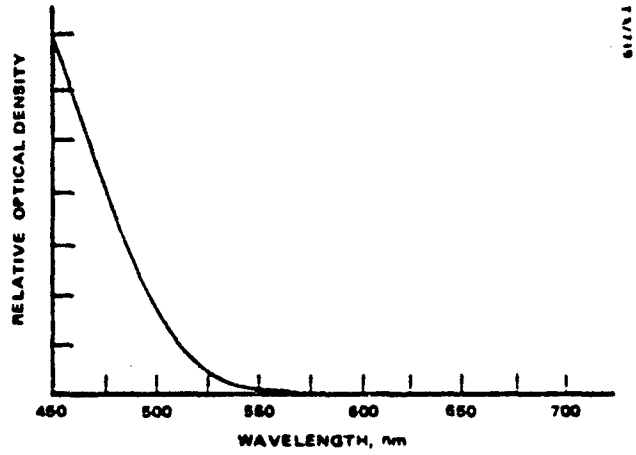

Figure 48. Absorption spectra of dichromate ions

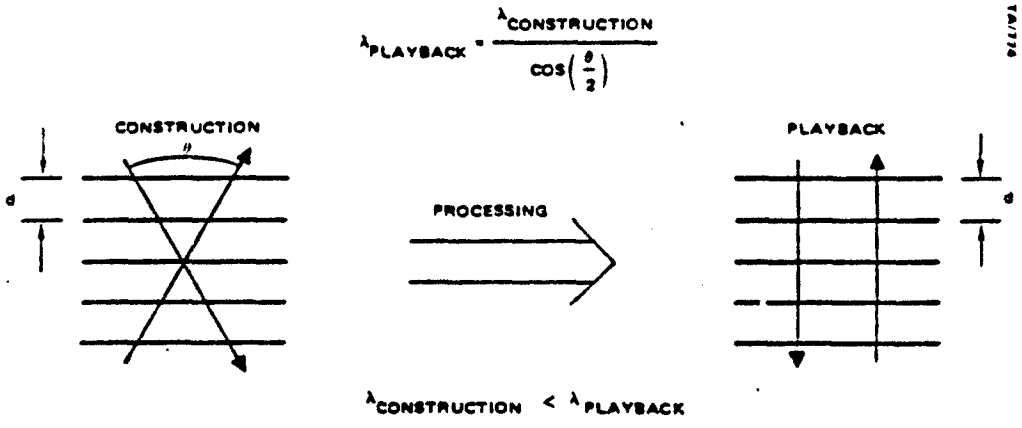

Figure 49. Results of changing construction geometry

5.0 1.06 μm HOLOGRAMS

5.2 FABRICATION OF 1.06 μm HOLOGRAMS

Fabrication of 1.06 μm holograms requires a special exposure apparatus to achieve the necessary construction angles and a modified gelatin to reach the desired efficiency level.

The 1.06 μm exposure apparatus makes use of two prisms to steer the laser beam into and out of the glass substrate. The prisms are necessary because the 61° incidence angle is greater than the critical angle for the air-glass interface. The construction set-up is shown in Figure 50. The input beam is steered through a 60° equilateral prism and the reflected beam exits through a 30-60-90 prism. The appropriate faces are AR coated to reduce multiple reflections. Careful alignment is required to prevent unwanted edge reflections from interfering with the desired hologram.

Since the hologram efficiency varies inversely as the wavelength, the dichromated gelatin must be modified to achieve the same efficiencies obtained at shorter wavelengths. The efficiency, η, can be written

$$\eta = \tanh^2 \left(\frac{\pi \Delta n \, d}{\lambda \cos \theta} \right)$$ where Δn is the index modulation and d is the gelatin thickness.

Therefore, for the same Δn the thickness of a 1.06 μm hologram must be twice that of a .53 μm hologram. The thicker gelatin is easily fabricated, but it introduces a new problem: the thicker gelatin has more dichromate ions and thus reduces the ratio of the output and input beams during exposure. A beam ratio nearly equal to one is necessary to obtain the high reflection efficiencies required for laser eye protection. By decreasing the dichromate concentration as a trade-off to improve the beam ratio, efficiencies up to 99.9% can be achieved at 1.06 μm. The gelatin thickness and dichromate concentration will need to be optimized to achieve high efficiencies consistently.

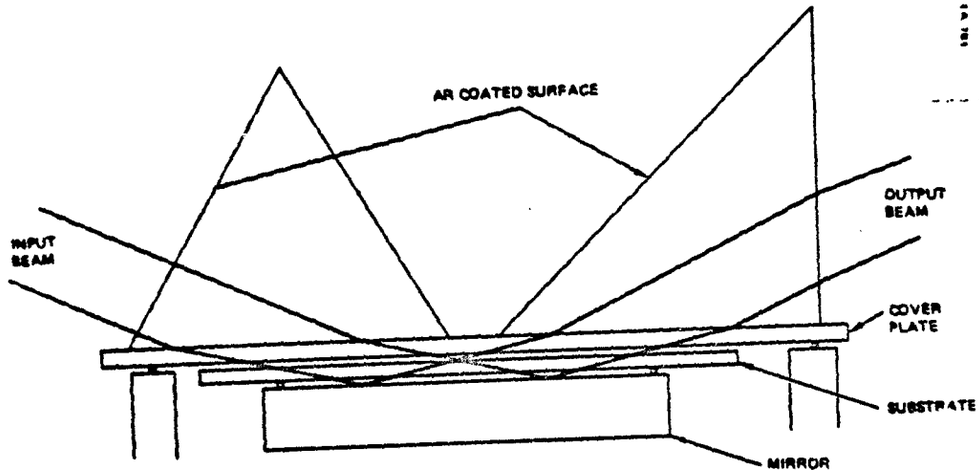

Figure 50. Exposure setup for 1.06μm hologram

5.0 1.06 μm HOLOGRAMS

5.3 1.06 μm HOLOGRAMS HAVE HIGH EFFICIENCY AND GOOD SEE-THROUGH

The holograms fabricated for 1.06 μm protection have achieved 99.8% reflection efficiency while maintaining a photopic transmission of 87%.

The maximum reflection efficiency for a single 1.06 μm hologram in this program is 99.8%. The peak wavelength is actually 1.09 μm, due to a shortened bakedown period. Figure 51 shows the efficiency versus wavelength plot for this hologram. An additional hologram at .545 μm was simultaneously fabricated with the desired hologram. This hologram comes from the first harmonic of the desired infrared wavelength.

The oblique construction angles required to obtain the necessary fringe spacing allow significant amounts of the input radiation to be reflected at the glass, oil, and gelatin interfaces. These reflections lower the efficiency of the hologram by reducing the beam ratio. In addition, the reflection at the gel-oil interface creates a low efficiency hologram which is spatially offset from the desired hologram. This additional hologram reduces the available index modulation and distorts the sinusoidal form of the fringes enough to allow the harmonics of the peak wavelength to be reflected also. Closer index matching of the gel, oil, and glass should eliminate these secondary holograms. However, the additional visible wavelength hologram can be an advantage when multiple wavelength protection is desired.

The photopic transmission for the 1.06 μm holograms is excellent, as expected for the narrow band rejection characteristics of reflection holograms. The table on the next page is a list of 1.06 μm plates and the corresponding efficiency and see-through measurements. The photopic transmission of the IR holograms is less than the theoretical maximum because of the .53 μm hologram. With the elimination of the hologram in the visible, the photopic transmission will be limited only by the gelatin absorption, which at present is approximately 3% at 1.06 μm.

Additional work must be done on the experimental process of varying the gelatin parameters, adjusting the processing techniques, and exposing at shorter wavelengths to reach the same high efficiencies which have been obtained at visible wavelengths with well-defined techniques. Two 1.06 μm holograms fabricated with the present techniques can be sealed together to yield efficiencies greater than 99.99%. Figure 52 shows the spectral scan for a double 1.06 μm hologram.

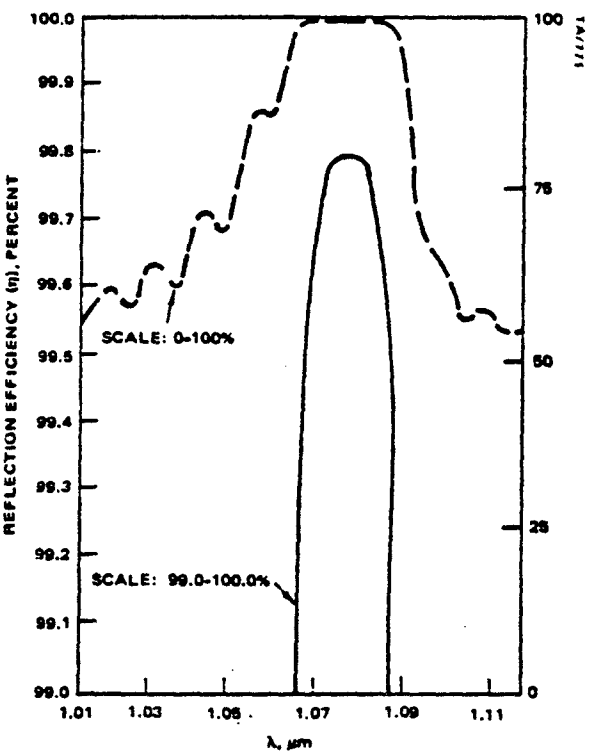

Figure 51. Single 1.06μm hologram

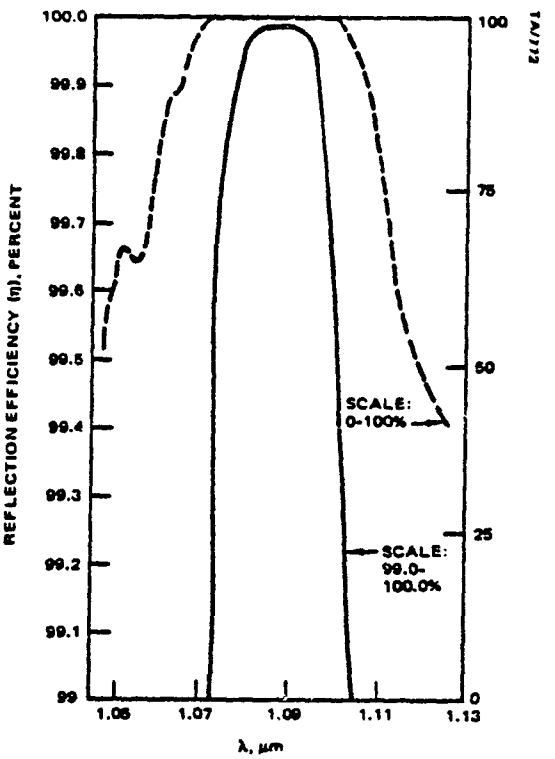

Figure 52. Druble 1.06μm hologram

TABLE OF INFRARED HOLOGRAMS

Sample Number	λ peak μm	η (%)	T (%)
180	1.125	99.6	91
220	1.105	99.8	85
199	1.075	99.8	87
208	1.110	99.4	91
197	1.140	99.0	96
204, 215	1.095	99.99	78
225, 227	1.110	99.99+	77
212, 222	1.095	99.98	79

6.0 MULTIPLE WAVELENGTH PROTECTION

6.1 MULTIPLE LAYERS PROVIDE MULTIPLE WAVELENGTH COVERAGE

Multiple layer holograms provide eye protection for more than one laser wavelength.

Multiple layer holograms provide better eye protection than multiple holograms in a single layer because of the finite amount of index modulation available in a single gelatin film. Figure 53 shows how multiple layers will allow greater index modulation for protection at each laser wavelength. The number of laser wavelengths protected by a multiple layer hologram is limited only by the photopic see-through requirements of the application. As more wavelengths in the visible region of the spectrum are rejected, the photopic transmission drops off rapidly.

To prove the multiple wavelength concept, a two wavelength hologram was fabricated to provide eye protection at an infrared laser wavelength and at a visible wavelength. As shown in Figure 54 the hologram protects .55 μm with an efficiency greater than 99.999% and 1.09 μm with 99.9% efficiency.

The total photopic transmission is 66%. The bandwidth and efficiency of the visible hologram limits the photopic see-through, so photopic transmission can be traded-off with additional protection at visible wavelengths. For the hologram in Figure 54, the bandwidth at .55 μm is 20.5 nm and at 1.09 μm is 1.0 nm. Therefore, the IR hologram does not affect the photopic transmission.

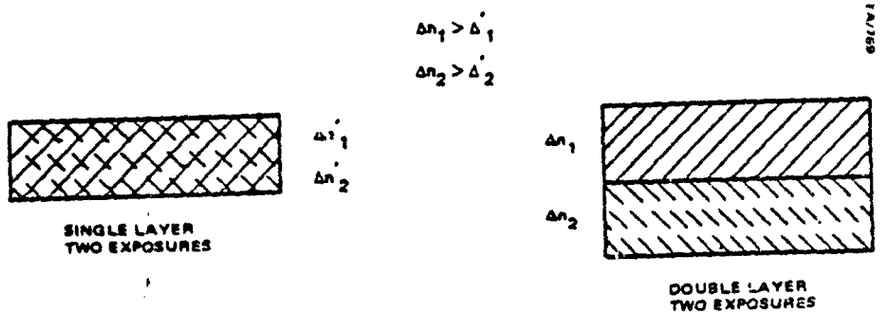

Figure 53. Multiple layers provide more index modulation for each wavelength

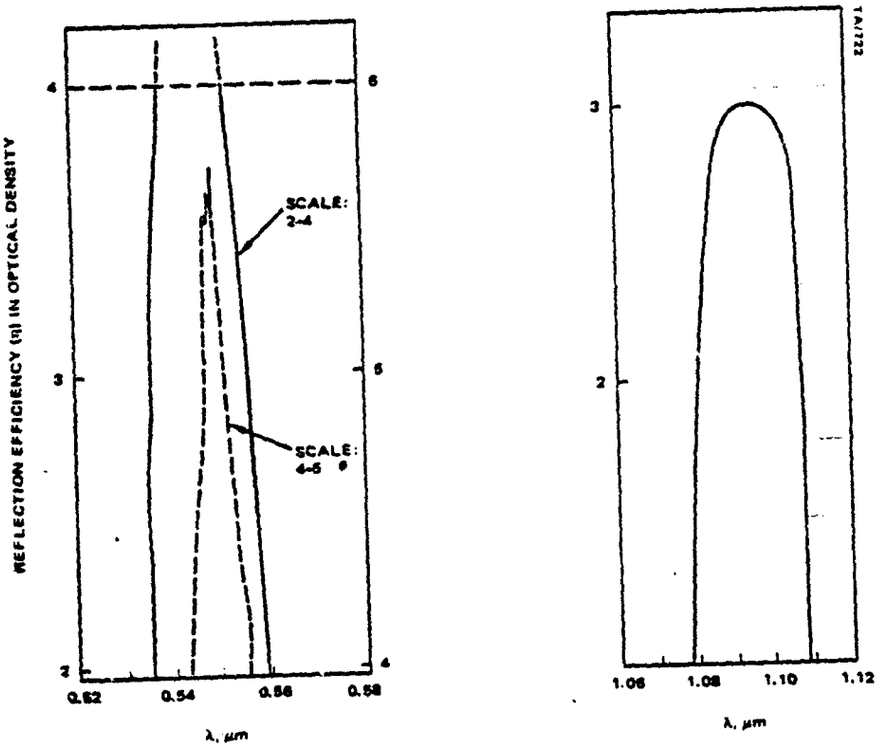

Figure 54. Efficiency of multilayer hologram

APPENDIX A

DETAILS OF EXPOSURE OPTICS AND PERFORMANCE OF INDIVIDUAL VISOR SEGMENTS

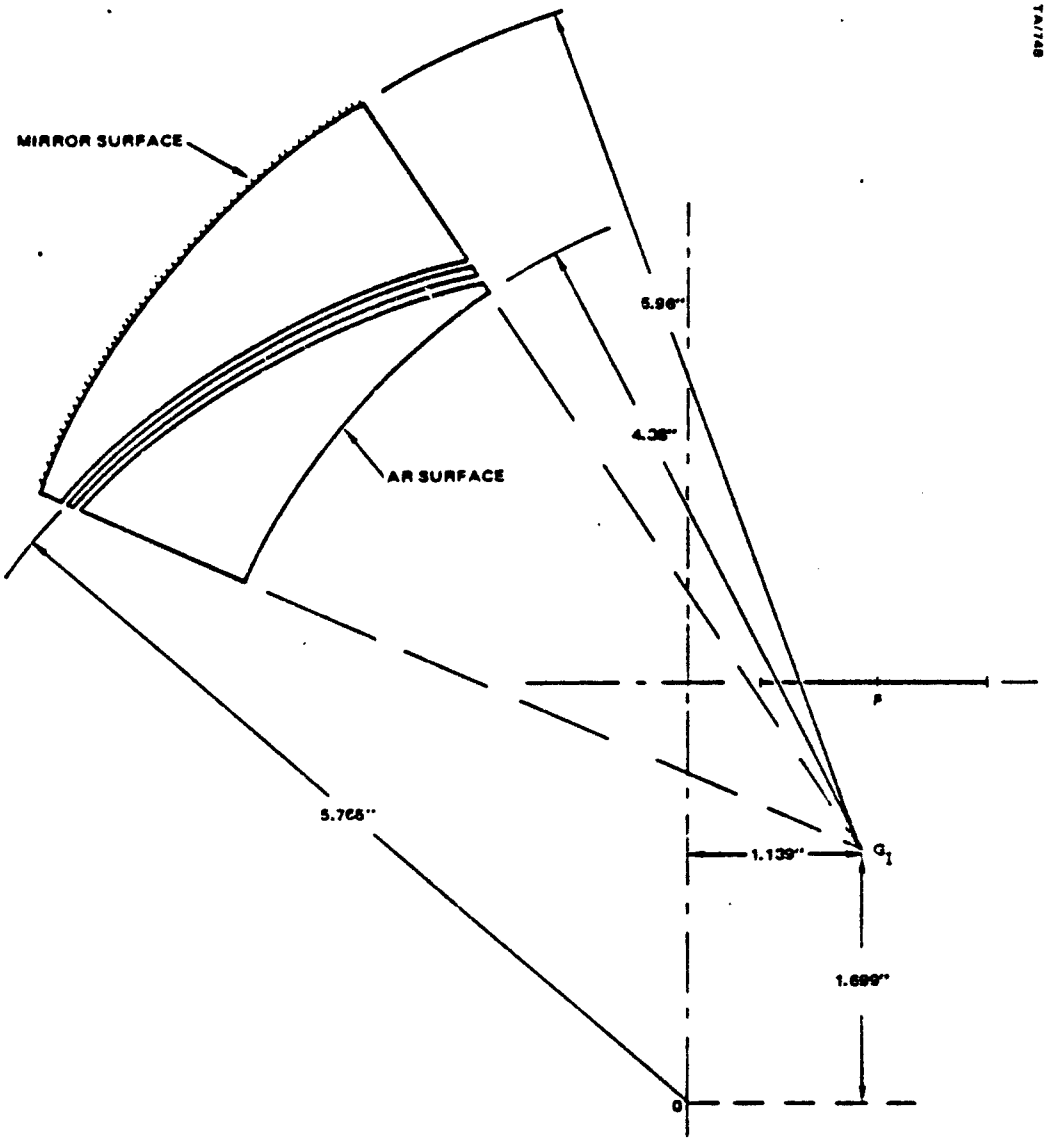

Figure A-1. Exposure optical setup for visor hologram I

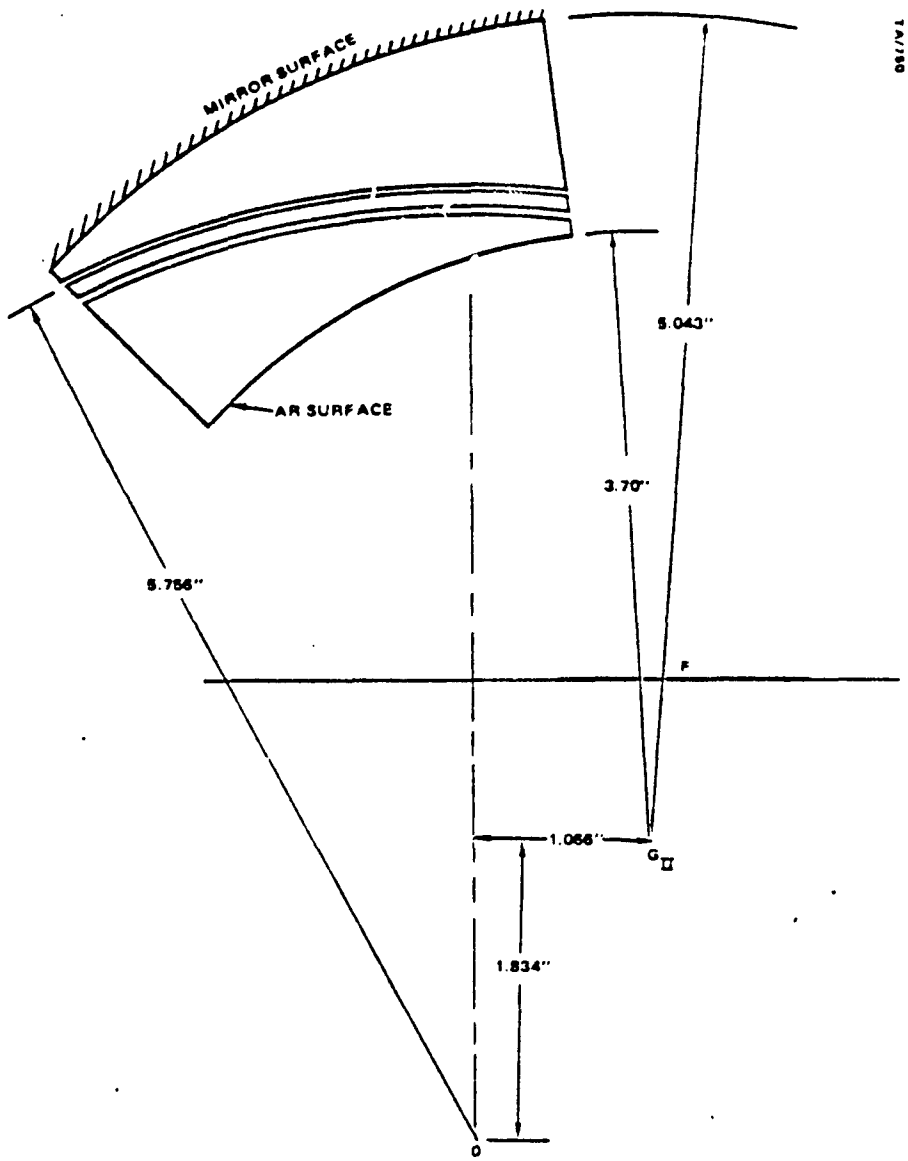

Figure A-2. Exposure optical setup for visor hologram II

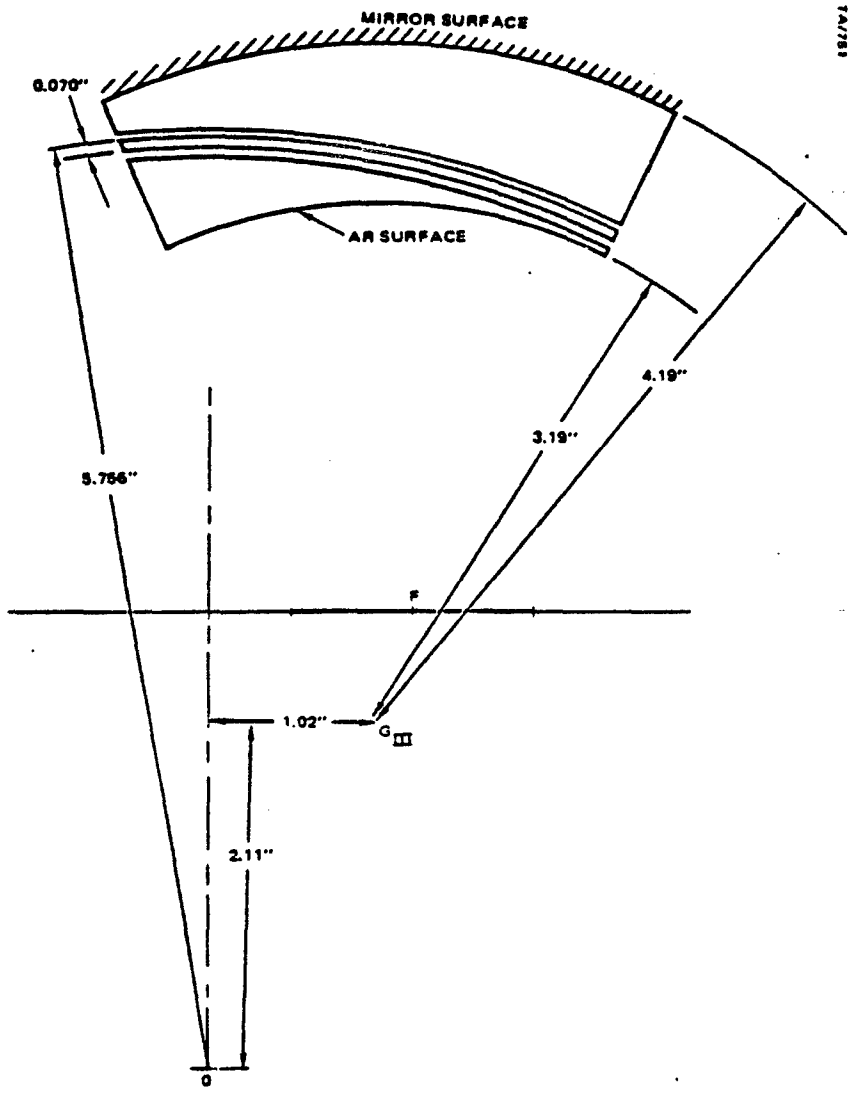

Figure A-3. Exposure optical setup for visor hologram III

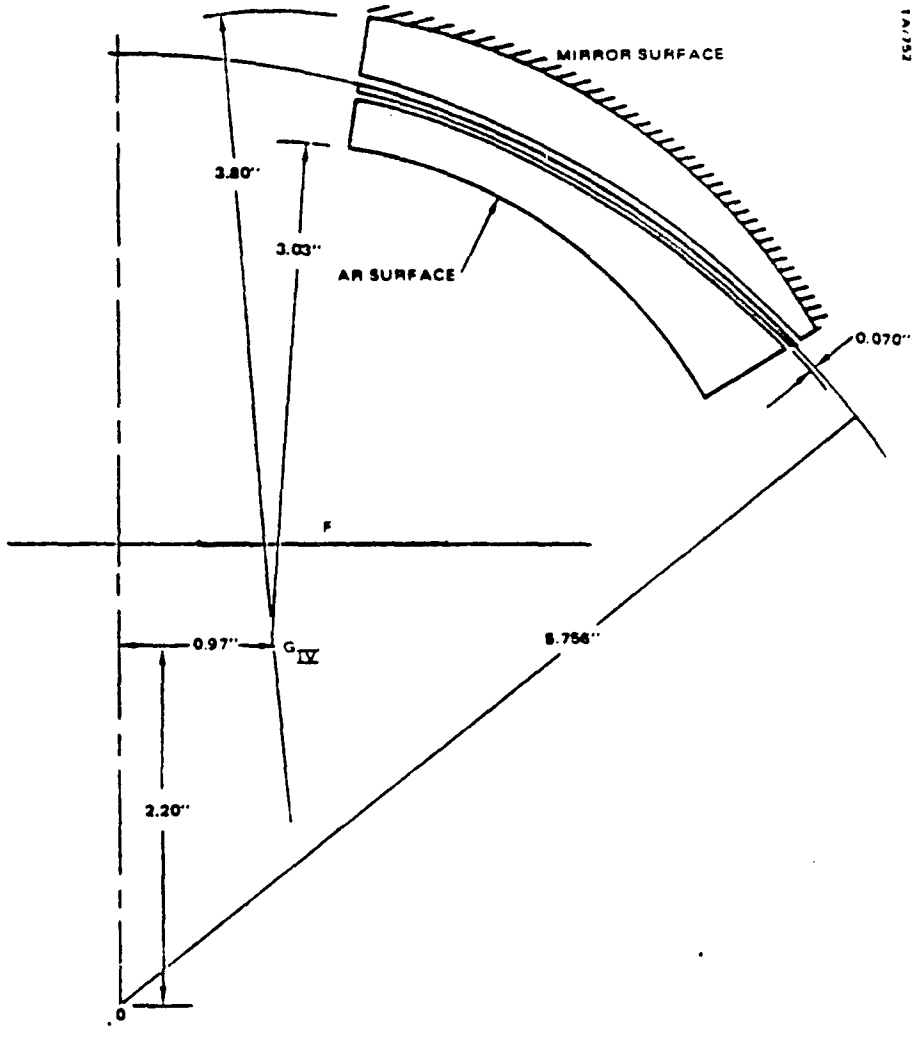

Figure A-4. Exposure optical setup for visor hologram IV

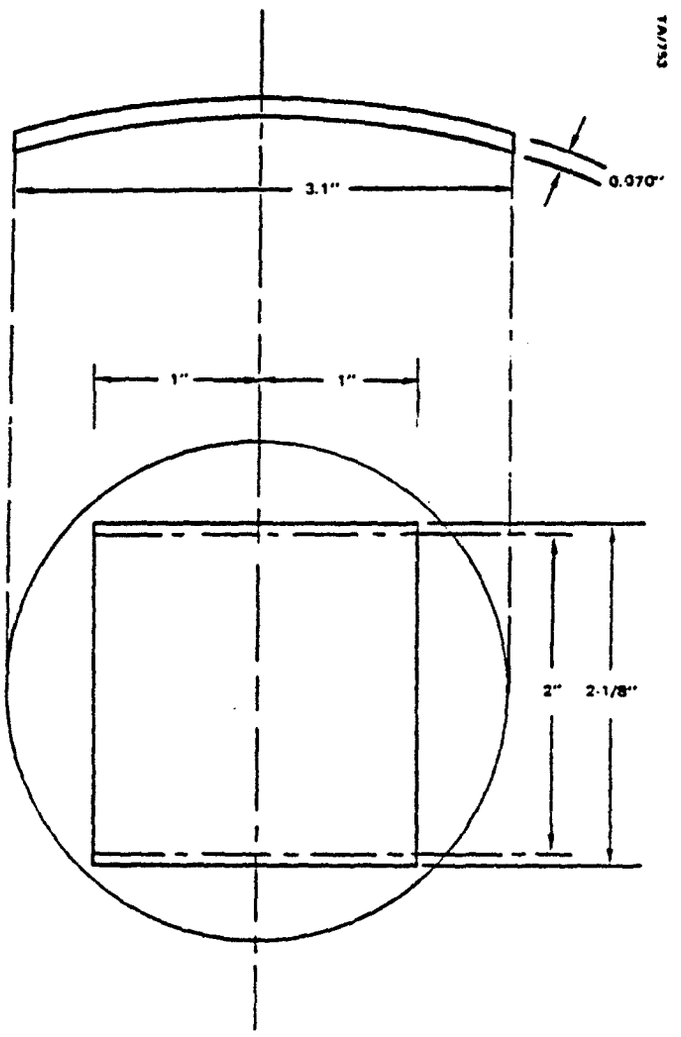

Figure A-5. Substrate dimensions for visor hologram (the center 2" x 2-1/8" portion is the useable area for visor mock-up)

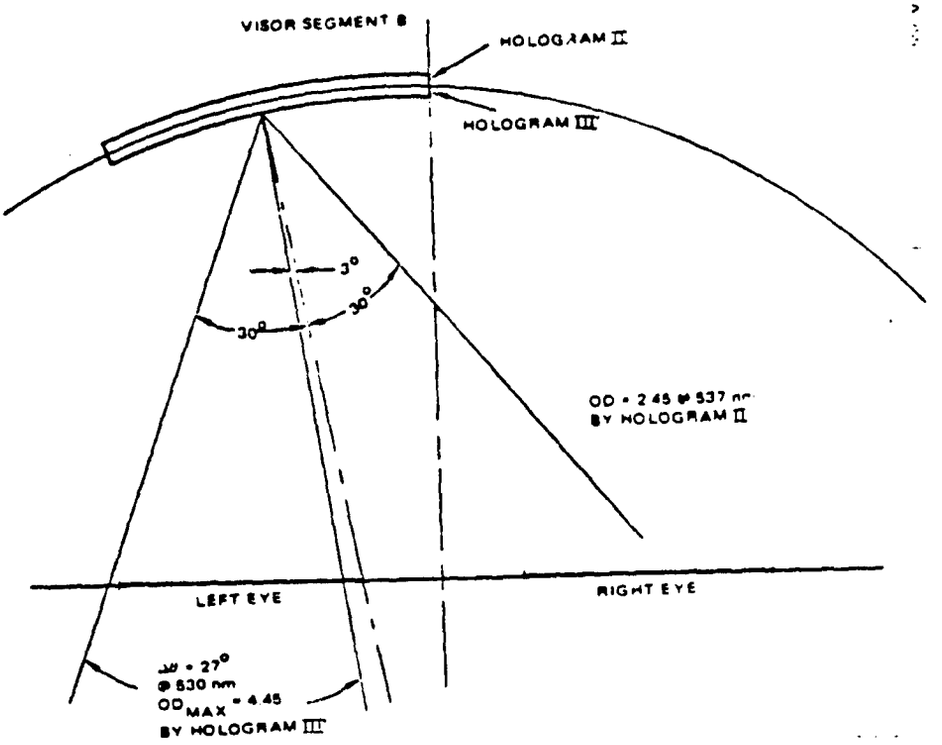

Figure A-6. Angular coverage at the center of visor segment B

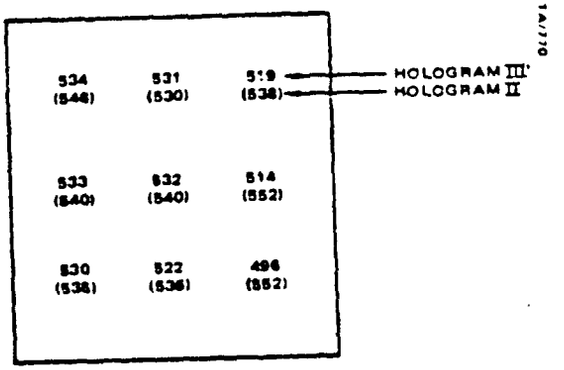

Figure A-7. Hologram wavelength variation at different positions on visor segment B

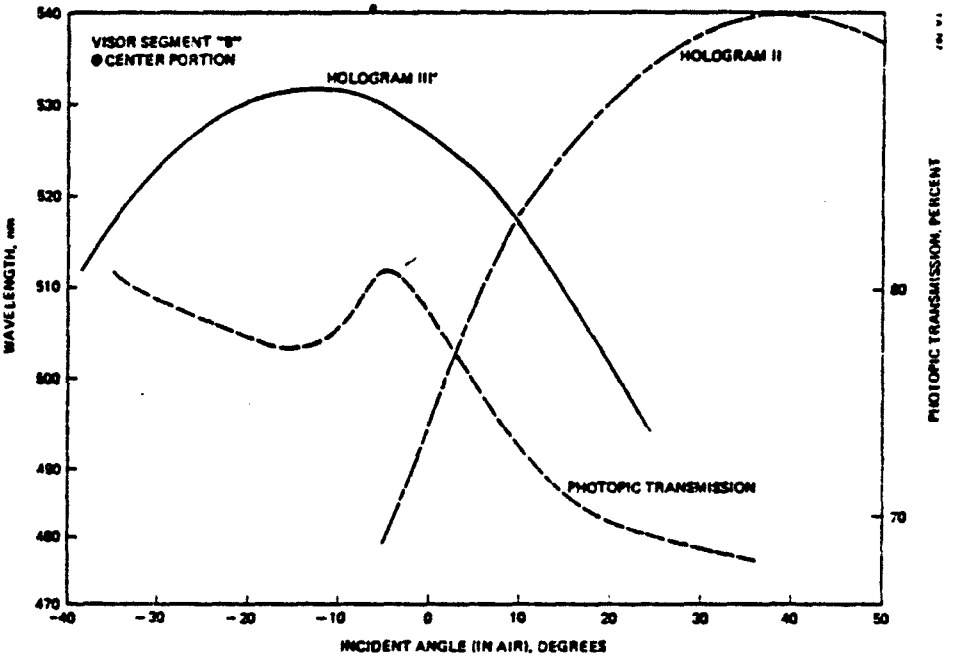

Figure A-8. Peak wavelength and photopic transmission as a function of incident angle for segment B

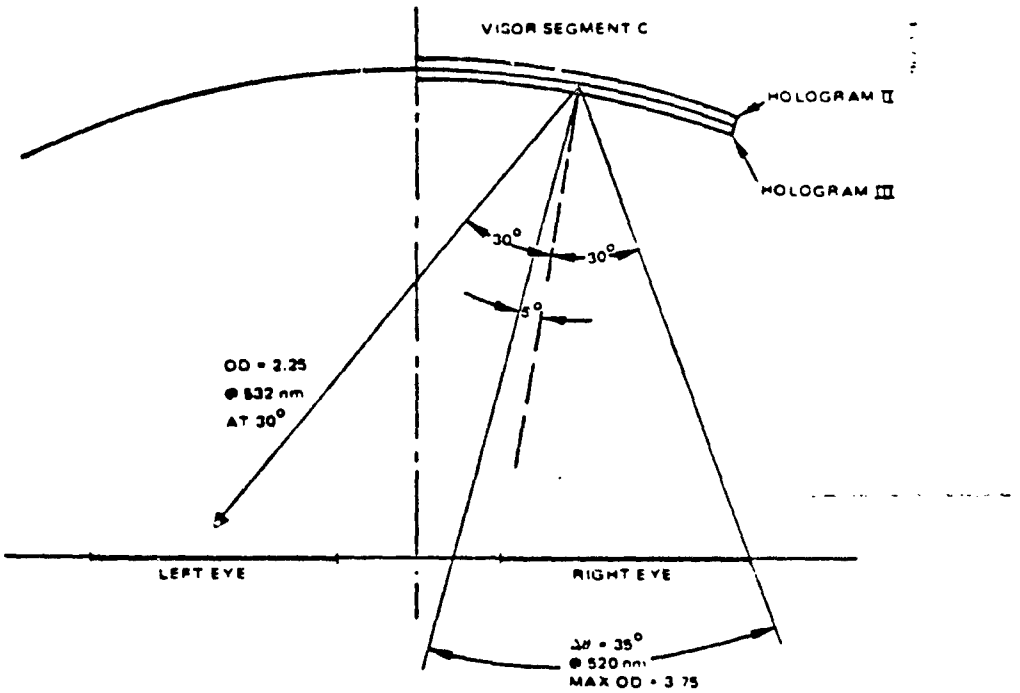

Figure A-9. Angular coverage at the center of visor segment C

504 (536)	521 (535)	520 (541)
534 (545)	530 (532)	540 ← HOLOGRAM III (531) ← HOLOGRAM II
513 (540)	527 (535)	527 (530)

Figure A-10. Hologram wavelength variation at different positions on visor segment C

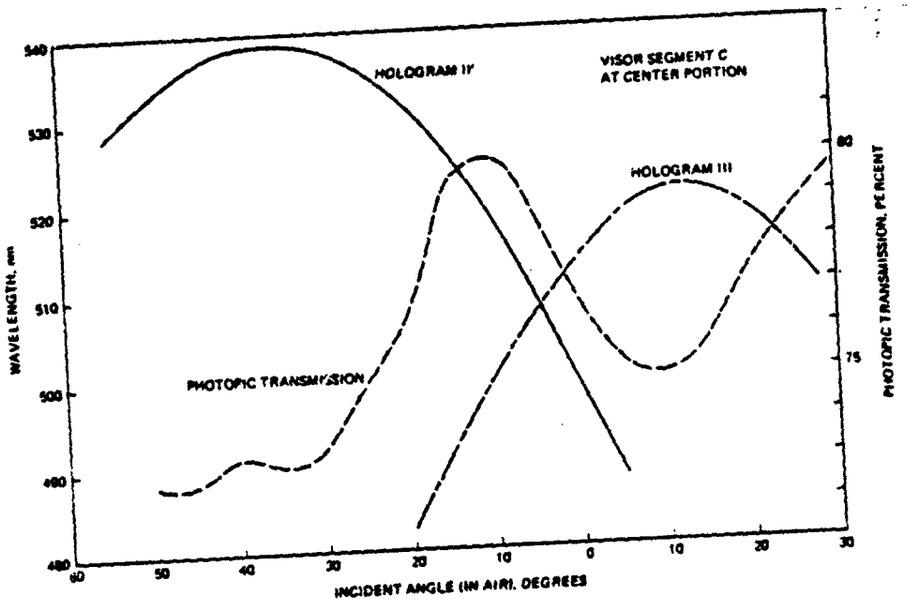

Figure A-11. Peak wavelength and photopic transmission as a function of incident angle for visor segment C

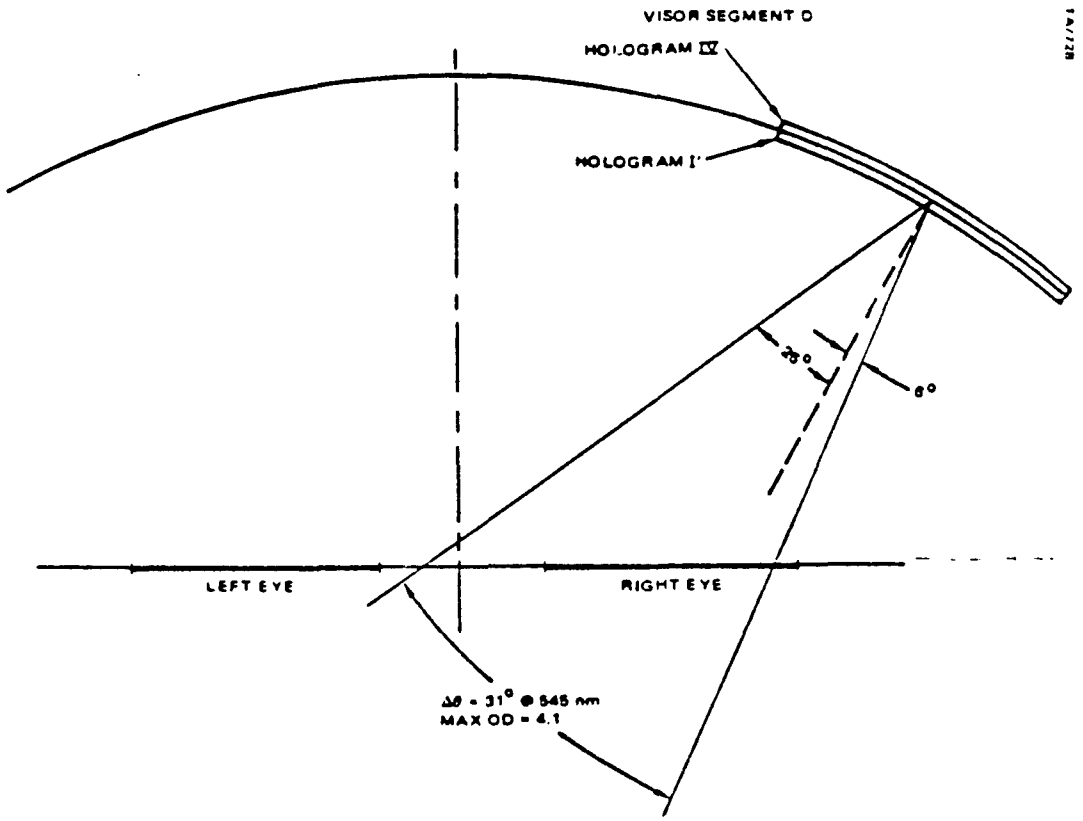

Figure A-12. Angular coverage at the center of visor segment D

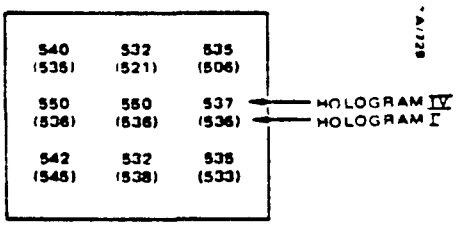

Figure A-13. Hologram wavelength variation at different positions on visor segment D

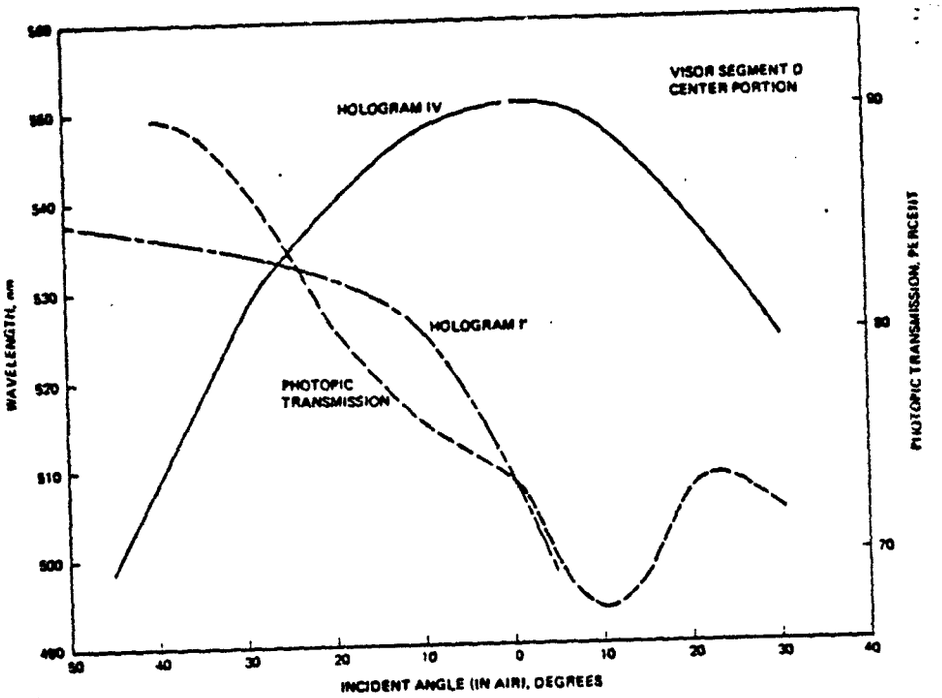

Figure A-14. Peak wavelength and photopic transmission as a function of incident angle for visor segment D

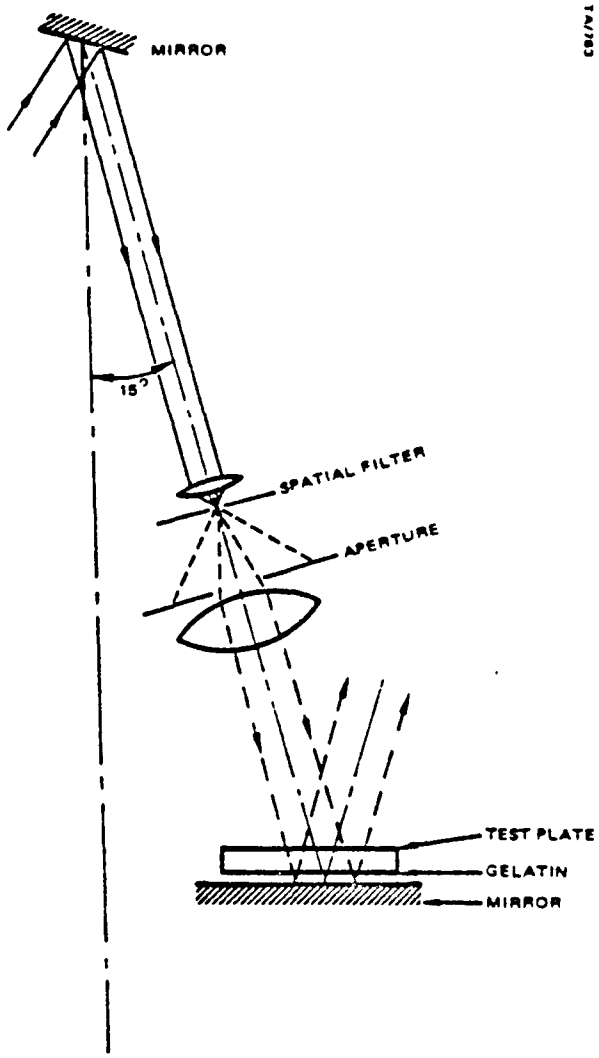

Figure A-15. Experimental exposure setup